The postcranial skeleton of the iguanodontian ornithopod *Jinzhousaurus yangi* from the Lower Cretaceous Yixian Formation of western Liaoning, China

Xiaolin Wang[1]*, Rui Pan[1], Richard J. Butler[2]* and Paul M. Barrett[3]

[1] Key Laboratory of Evolutionary Systematics of Vertebrates, Institute of Vertebrate Paleontology and Paleoanthropology, Chinese Academy of Sciences, PO Box 643, Beijing, 100044, China
Email: wangxiaolin@ivpp.ac.cn; panrui@ivpp.ac.cn

[2] Bayerische Staatssammlung für Paläontologie und Geologie, Richard-Wagner-Straße 10, 80333 Munich, Germany
Email: butler.richard.j@gmail.com

[3] Department of Palaeontology, The Natural History Museum, Cromwell Road, London SW7 5BD, UK
Email: P.Barrett@nhm.ac.uk

*Corresponding authors

ABSTRACT: Non-hadrosaurid iguanodontians were the most diverse and abundant group of large-bodied herbivorous dinosaurs during the Early Cretaceous, and were a particularly important component of Laurasian ecosystems. Recent years have seen a dramatic increase in our knowledge of the diversity of this group, with multiple new taxa being described from northeast China. The most complete of these Chinese non-hadrosaurid iguanodontians is *Jinzhousaurus yangi*, from the middle part of the Yixian Formation (Lower Cretaceous: lower Aptian) of Liaoning Province. Here, we provide the first description of the relatively complete and partially articulated postcranial skeleton of the holotype of *Jinzhousaurus*, and provide detailed comparisons to closely related taxa. We document additional autapomorphies of *Jinzhousaurus* that provide strong support for the validity of this taxon.

KEY WORDS: Early Cretaceous, Iguanodontia, Ornithopoda, Hadrosauridae, systematics

Iguanodontia is an important clade of medium- to large-bodied herbivorous ornithopod dinosaurs that includes the largely Late Cretaceous hadrosaurids and a series of more basal taxa Jurassic and Cretaceous taxa, including *Iguanodon*, *Camptosaurus*, *Dryosaurus* and *Tenontosaurus* (e.g., Sereno 1986, 1999; Norman 1990, 1998, 2002, 2004, in press; Weishampel *et al.* 2003; You *et al.* 2003). The term 'non-hadrosaurid iguanodontian' will be used in the present paper to refer to a paraphyletic assemblage of ornithopod taxa than excludes Hadrosauridae. (Paul (2008) recently used the term iguanodont for a similar taxonomic grouping.) Although not a monophyletic grouping, non-hadrosaurid iguanodontians represent an organisational grade intermediate between hadrosaurids and more basal 'hypsilophodontid' ornithopods (e.g., Norman 2004). Non-hadrosaurid iguanodontians originated in the Middle Jurassic (*Callovosaurus leedsi*); however, as is generally the case for ornithopods, they did not form a significant component of ecosystems at a global level until the Cretaceous (Weishampel *et al.* 2004). During the Early and mid Cretaceous they became the most diverse and abundant group of medium to large-bodied herbivorous dinosaurs, but they declined in the Late Cretaceous as hadrosaurids diversified (Norman 2004).

In the last decade our understanding of the diversity of non-hadrosaurid iguanodontians has increased dramatically, with the description of new taxa from several continents, including North America (Head 1998; Kirkland 1998), Europe (Mateus & Antunes 2001; Dalla Vecchia 2009; Norman in press), South America (e.g. Novas *et al.* 2004; Calvo *et al.* 2007), and Africa (Taquet & Russell 1999). However, the greatest diversity of new taxa has been described from the upper Lower Cretaceous deposits of northern and northeastern China (Table 1, Fig. 1), including '*Probactrosaurus*' *mazongshanensis* (inverted commas indicate that the generic attribution of this species is uncertain: Norman 2002) from the Xinminbao Group (Barremian–Albian) of Gansu Province (Lü 1997), *Equijubus normani*, also from the Xinminbao Group of Gansu (You *et al.* 2003a), *Nanyangosaurus zhugeii*, from the Sangping Formation (?Albian) of Henan Province (Xu *et al.* 2000), *Penelopognathus weishampeli* from the Bayan Gobi Formation (Albian) of Inner Mongolia (Nei Monggol Autonomous Province: Godefroit *et al.* 2005), *Shuangmiaosaurus gilmorei* from the Sunjiawan Formation (Cenomanian–Turonian) of Liaoning Province (You *et al.* 2003b), and *Lanzhousaurus magnidens*, from the Hekou Group (Lower Cretaceous) of Gansu Province (You *et al.* 2005). Finally, Wang & Xu (2001a, b) erected *Jinzhousaurus yangi* on the basis of a nearly complete, partially articulated skull and skeleton collected from the middle part of the Yixian Formation (Jehol Group: lower Aptian) of Liaoning Province. *Jinzhousaurus yangi* is highly significant in that its holotype specimen is the most complete non-hadrosaurid iguanodontian specimen known from Asia. No other specimens referable to *Jinzhousaurus* have yet been described from the Yixian Formation,

 doi:10.1017/S1755691010009266

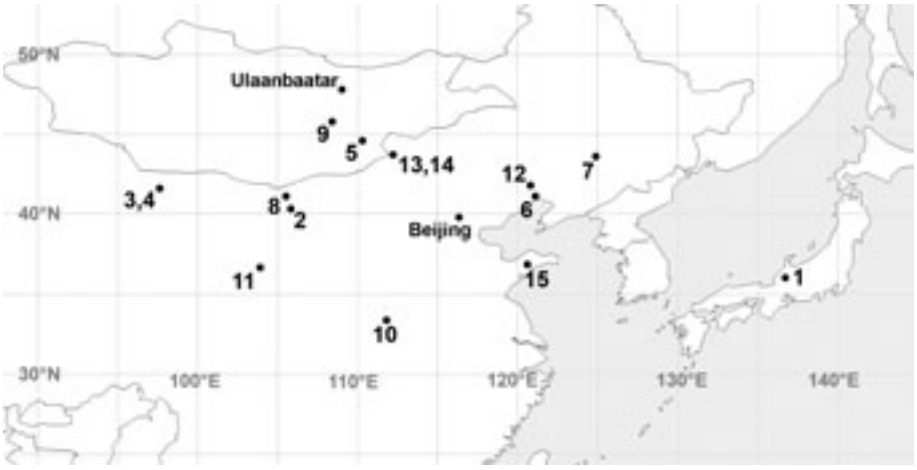

Figure 1 Main localities for non-hadrosaurid iguanodontians in East Asia. See Table 1 for details. *Jinzhousaurus yangi* is from locality 6.

although indeterminate non-hadrosaurid iguanodontian remains have been reported from the overlying Jiufotang Formation (Xu & Norell 2006).

The original description of *Jinzhousaurus* focused only on the skull (Wang & Xu 2001a, b); however, the postcranial skeleton has since been prepared and is well preserved, partially articulated and nearly complete. Barrett *et al*. (2009) provided an extensive redescription of the skull of *Jinzhousaurus*, as well as a rediagnosis that focused on cranial characters. In the present paper, the authors provide the first description of the postcranial skeleton and compare it in detail to other penecontemporaneous and closely related taxa. Additional postcranial autapomorphies that support the validity of *Jinzhousaurus* are recognised and described.

Institutional abbreviations: NHMUK, Natural History Museum, London; IRSNB, Institute Royal des Sciences Naturalle de Belgique, Brussell, Belgium; IVPP, Institute of Vertebrate Paleontology and Paleoanthropology, Chinese Academy of Sciences, Beijing.

1. Systematic palaeontology

Ornithischia Seeley, 1887
Ornithopoda Marsh, 1881
Iguanodontia Sereno, 1986
Iguanodontoidea Cope, 1869 (*sensu* Norman 2002)
? Hadrosauroidea Cope, 1869 (*sensu* Sereno 1998)

Jinzhousaurus yangi Wang & Xu, 2001a

Holotype. IVPP V12691, a largely complete individual comprising the skull and most of the postcranial skeleton (Wang & Xu 2001a, b, figs 1, 2; Barrett *et al*. 2009, figs 1–3) (Figs 2–9).

Type locality and horizon. Baitaigou, Toutai Town, Yixian County, Liaoning Province, People's Republic of China (Fig. 1). The specimen comes from the Dakangpu Member (equivalent to the Dawangzhangzi Bed or Member) of the middle Yixian Formation (Wang & Zhou 2003), which has been dated as Lower Cretaceous (lower Aptian) in age (Smith *et al*. 1995; Swisher *et al*. 1999, 2002).

Revised diagnosis. Differs from all other non-hadrosaurid iguanodontians in possessing the following autapomorphies: large shallow fossa present on the anterior part of the maxilla adjacent to the premaxillary junction; lachrimal reduced in size with a sub-triangular outline; nasals terminate in a pointed, sub-triangular posterior process that overlaps the frontals; frontal unit with a 'T'-shaped outline in dorsal view and prominent, distinct postorbital processes that are offset from the main body of the bone; laterodorsal surface of the frontal bears an elongate shallow depression; predentary with unilobate midline process that expands in transverse width distally; sternal bears a well-developed, posteriorly positioned, tab-like midline process that forms an angle of approximately 80 degrees with the posterolateral process; manual phalanx III-1 is broader than long and less than 20% the length of metacarpal III (modified from Barrett *et al*. 2009).

Comments. The postcranial skeleton of the holotype specimen was unprepared at the time of the initial description and all of the diagnostic features listed were restricted to the skull (Wang & Xu 2001a, b). However, as discussed by Barrett *et al*. (2009), most of the features mentioned in the original diagnosis have a much wider distribution among non-hadrosaurid iguanodontians. Barrett *et al*. (2009) proposed a revised diagnosis based upon cranial anatomy only, and moreover discussed inaccuracies present in an emended diagnosis for the genus proposed by Paul (2008). The present authors propose two additional postcranial autapomorphies for *Jinzhousaurus*, which are discussed in greater detail in the text. Moreover, they provide detailed comparisons to other non-hadrosaurid iguanodontian taxa for which postcranial material is known.

2. Description and comparisons

2.1. Overview

The skeleton was collected from a single bedding plane in a number of slabs that have subsequently been embedded in plaster in approximately the positions in which they were recovered (Fig. 2). The skull slab, which also contains the first seven cervical vertebrae, is kept separately, and a cast of this slab is mounted along with the postcranial skeleton. Most of the postcranium is divided between two large plaster blocks containing the anterior and posterior portions of the skeleton. In addition to the cast of the skull slab, the anterior block includes the remaining cervical vertebrae in articulation, a series of disarticulated dorsal vertebral centra and some more complete dorsal vertebrae, a series of articulated dorsal ribs, a partial sacrum, both pectoral girdles and forelimbs, including both manus, and a number of ossified tendons. The posterior block contains the posterior part of the skeleton and includes a small part of the posterior end of the sacrum, a partially articulated tail, ossified tendons, the pelvic girdle, and partial

Table 1 Non-hadrosaurid iguanodontians of East Asia (see Fig. 1). Some of these taxa (e.g. *Tanius*) have been previously considered hadrosaurids, but are placed outside of Hadrosauridae by recent phylogenetic analyses (e.g. Prieto-Marquez & Wagner 2009; Prieto-Marquez 2010).

	Taxon and reference	Location	Formation	Age	Material
1	*Fukuisaurus tetoriensis* (Kobayashi & Azuma 2003)	Kitadani, Fukui Prefecture, Japan	Kitadani	late Hauterivian–Barremian	Disarticulated cranial material and sternal plates
2	*Probactrosaurus gobiensis* (Norman 2002)	Maortu, Inner Mongolia, China	Dashuigou	Barremian–Albian	Partial skull and postcranial skeleton
3	'*Probactosaurus*' *mazongshanensis* (Lü 1997)	Mazongshan, Gansu, China	Xinminbao Group	Barremian–Aptian	Partial skull and postcranial skeleton
4	*Equijubus normani* (You *et al.* 2003a)	Mazongshan, Gansu, China	Xinminbao Group	Barremian–Aptian	Partial skull and postcranial skeleton
5	*Iguanodon bernissartensis* (= '*I. orientalis*': Norman 1996)	Khamarin-Khural, Dornogov, Mongolia	Unnamed	Barremian–Aptian	Fragmentary cranial and postcranial elements
6	***Jinzhousaurus yangi***	Baicaigou, Liaoning, China	Yixian	early Aptian	Near complete skull and partially articulated postcranial skeleton
7	Iguanodontia indet. (Chen *et al.* 2008)	Liufangzi, Jilin, China	Quantou	Aptian–Cenomanian	Humerus
8	*Penelopognathus weishampeli* (Godefroit *et al.* 2005)	Qiriga, Inner Mongolia, China	Bayan Gobi	Albian	Dentary
9	*Altirhinus kurzanovi* (Norman 1998)	Huren-duh, Dornogov, Mongolia	Khuren Dukh	late Aptian–early Albian	Complete skull, additional cranial and postcranial material
10	*Nanyangosaurus zhugeii* (Xu *et al.* 2000)	Neixing County, Henan, China	Sangping	Early Cretaceous: ?Albian	Partial postcranial skeleton
11	*Lanzhousaurus magnidens* (You *et al.* 2005)	Zhongpu, Gansu, China	Hekou	Early Cretaceous	Mandible, teeth, vertebrae, sterna plates, pubes
12	*Shuangmiaosaurus gilmorei* (You *et al.* 2003b)	Shuangmiao, Liaoning, China	Sunjiawan	Cenomanian–Turonian	Maxilla and dentary
13	*Bactrosaurus johnsoni* (Godefroit *et al.* 1998)	Iren Dabashu/Erenhot, Inner Mongolia, China	Iren Dabashu	Late Cretaceous	Disarticulated cranial and postcranial material of multiple individuals
14	*Gilmoreosaurus mongoliensis* (Gilmore 1933)	Iren Dabashu, Inner Mongolia, China	Iren Dabashu	Late Cretaceous	Disarticulated cranial and postcranial material of multiple individuals
15	*Tanius sinensis* (Wiman 1929)	Laiyang, Shandong, China	Wangshi Group	?Coniacian–?Maastrichtian	Cranial and postcranial material

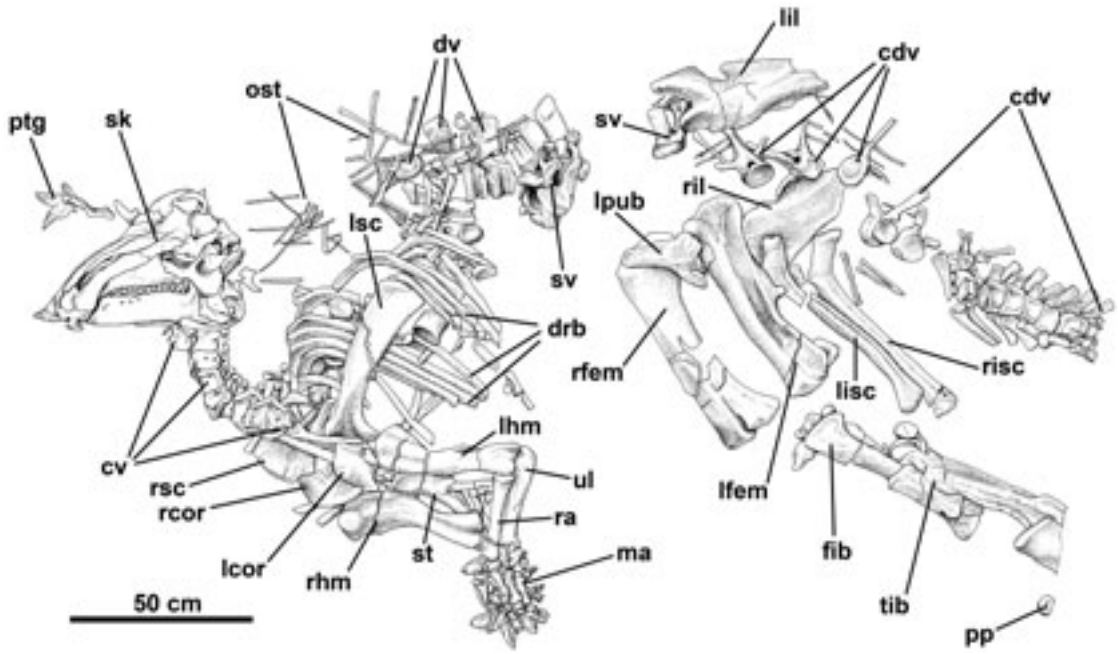

Figure 2 *Jinzhousaurus yangi*, IVPP V12691 (holotype). Skull and partially articulated postcranial skeleton. The specimen is mounted as two anterior and posterior blocks. Abbreviations: cdv=caudal vertebrae; cv=cervical vertebrae; drb=dorsal ribs; dv=dorsal vertebrae; fib=fibula; lcor=left coracoid; lfem=left femur; lhm=left humerus; lil=left ilium; lisc=left ischium; lpub=left pubis; lsc=left scapula; ma=left and right manus; ost=ossified tendons; pp=pedal phalanx; ptg=pterygoid; ra=radius; rcor=right coracoid; rfem=right femur; rhm=right humerus; ril=right ilium; risc=right ischium; rsc=right scapula; sk=skull; st=sternum; sv=sacral vertebrae; tib=tibia; ul=ulna. Scale bar=50 cm.

hindlimbs lacking the pedes. The skeleton has undergone severe compression, so that the leg and pelvic material has been extensively crushed, and the two forelimbs overlie each other with the hands pressed together in a supinated posture. There do not appear to be any preserved soft tissues associated with the skeleton. As preserved, the specimen is approximately 3·3 m long from the tip of the snout to the end of the proximal tail section. A small amount (approximately 200 mm) of this length has to be deducted, as the blocks are not in natural articulation, and it is likely that the additional tail vertebrae would have added around another 2 m to the length (based upon comparisons with other non-hadrosaurid iguanodontians; Norman 2004); the body length of the holotype is estimated at around 5–5·5 m.

Comparisons are made to other non-hadrosaurid ankylopollexian iguanodontians for which postcranial material is known, based upon published descriptions of *Altirhinus kurzanovi* (Norman 1998), *Camptosaurus* spp. (Gilmore 1909; Carpenter & Wilson 2008), *Eolambia caroljonesa* (Kirkland 1998), *Equijubus normani* (You *et al*. 2003a), *Fukuisaurus tetoriensis* (Kobayashi & Azuma 2003), *Iguanodon bernissartensis* (Norman 1980), *Lanzhousaurus magnidens* (You *et al*. 2005), *Lurdusaurus arenatus* (Taquet & Russell 1999), *Nanyangosaurus zhugeii* (Xu *et al*. 2000), *Ouranosaurus nigeriensis* (Taquet 1976), *Probactrosaurus gobiensis* (Norman 2002), '*Probactosaurus*' *mazongshanensis* (Lü 1997), and *Tethyshadros insularis* (Dalla Vecchia 2009). Comparisons could not be made to *Penelopognathus weishampeli* or *Shuangmiaosaurus gilmorei*, because these taxa are known only from cranial material (You *et al*. 2003b; Godefroit *et al*. 2005), while comparisons to *Protohadros byrdi* are also very limited, as little postcranial material is known (partial atlas, single ungual phalanx, ribs; Head 1998).

Norman (1986) provided a detailed description of the osteology of '*Iguanodon*' *atherfieldensis*, based largely upon a nearly complete referred skeleton from Belgium (IRSNB 1551). Recently, Paul (2008) has made this specimen the holotype of a new genus and species, *Dollodon bampingi*. Moreover, Paul (2006) erected the new genus *Mantellisaurus* for the species '*I*. *atherfieldensis*. Although the present authors believe that these taxonomic revisions require validation based upon direct examination of specimens, they are provisionally accepted herein. Comparisons to *Dollodon bampingi* are therefore based upon published descriptions of IRSNB 1551 (primarily Norman 1986), while comparisons to *Mantellisaurus atherfieldensis* are based upon the type specimen, NHMUK R5764, as described by Hooley (1925) and Norman (1986). NHMUK R5764 is currently mounted in the dinosaur gallery of the Natural History Museum (London) in such a way that detailed first-hand examination of this specimen was not possible as part of this present study.

2.2. Axial skeleton

2.2.1. Atlas. The left neural arch of the atlas is preserved adjacent to the left quadratojugal (Fig. 3a: at); the right neural arch is present on a separate block. Neither the intercentrum nor the odontoid process are visible, and may be obscured by the overlying skull. Both neural arches are preserved in lateral view. The neural arch consists of a vertically oriented stout pedicle that is anteroposteriorly expanded ventrally. This pedicle supports the pre- and postzygapophyses: there is no neural spine. The prezygapophysis is a robust, dorsoventrally deep, anteriorly directed process that terminates in a bluntly rounded, rugose tip (Fig. 3a: atprz). It is transversely broader than the postzygapophysis, which extends posteriorly and slightly dorsally as a slender tapering process in lateral view (Fig. 3a: atpoz). The ventral surface of the postzygapophysis is grooved, forming a facet for articulation with the axial neural arch. Anteromedial to the postzygapophysis the medial edge of the arch and prezygapophysis is drawn out into a medially extending, dorsoventrally compressed flange that would have approached its neighbour above the atlantal intercentrum.

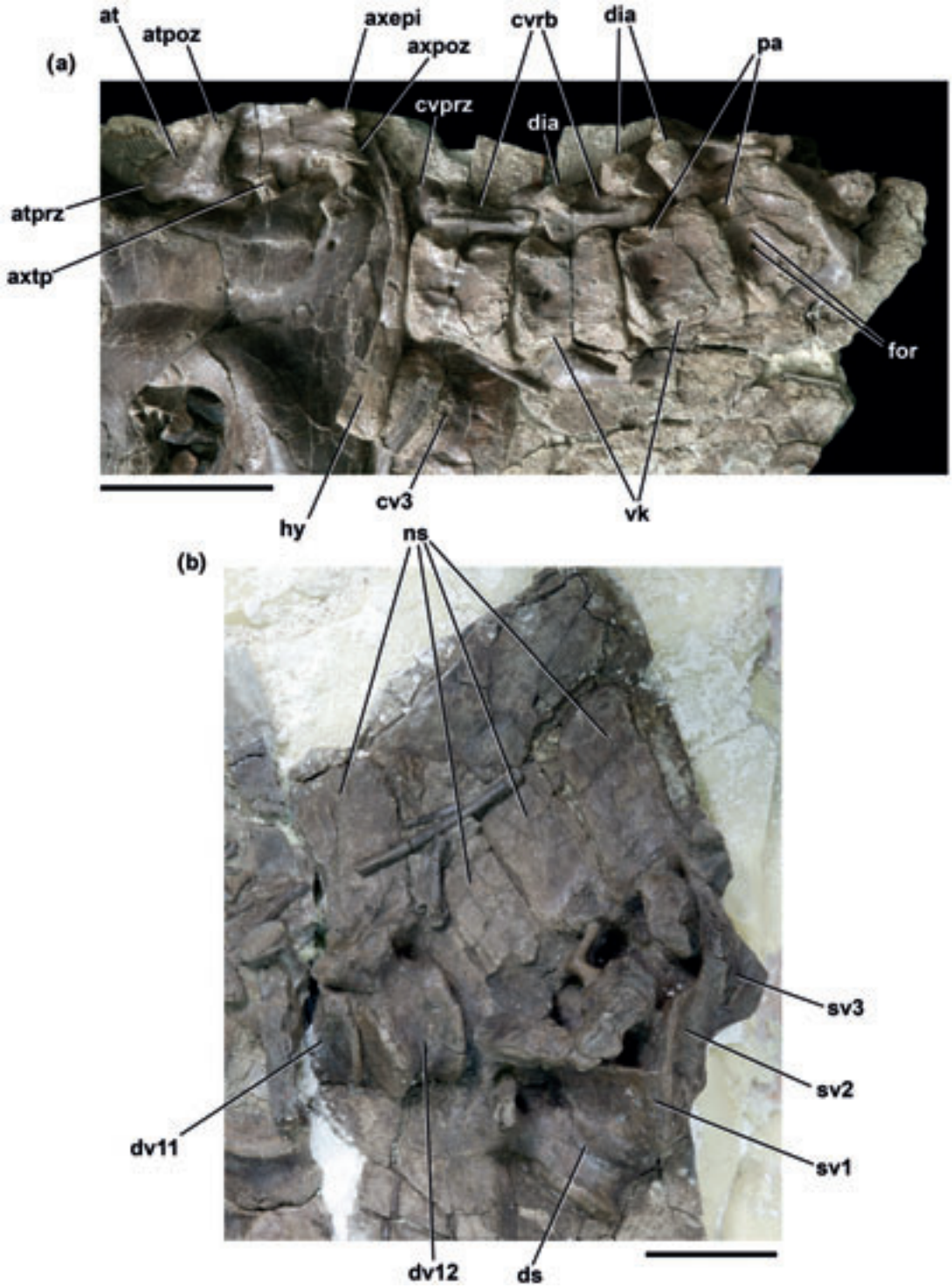

Figure 3 *Jinzhousaurus yangi*, IVPP V12691 (holotype): (a) Cervical vertebrae 1–7, preserved on slab with skull. Only parts of the atlas and axis are visible, and cervical 3 is visible only in ventral view. A small fragment of cervical 8 is also present; (b) Two most posterior dorsal vertebrae and anterior sacral vertebrae. Abbreviations: at=atlantal neural arch; atpoz=postzygapophysis of atlas; atprz=prezygapophysis of atlas; axepi=epipophysis of axis; axpoz=postzygapophysis of axis; axtp=transverse process of axis; cv3=cervical vertebra 3; cvprz=prezygapophysis of cervical vertebra; cvrb=cervical ribs; dia=diapophysis; ds=dorsosacral vertebra; dv11, dv12=dorsal vertebrae '11' and '12'; for=foramina; hy=hyoid; ns=neural spines; pa=parapophysis; sv1, sv2, sv3=sacral vertebrae; vk=ventral keel. Scale bars=10 cm.

The incomplete exposure of the atlas limits anatomical comparisons, but the element does not appear to differ significantly from that of other non-hadrosaurid iguanodontians (e.g., *Altirhinus kurzanovi*, Norman 1998, fig. 23; *Iguanodon bernissartensis*, Norman 1980, figs 22–23).

2.2.2. Axis. The neural arch of the axis is visible in left lateral view, situated next to the quadratojugal and posterior end of the mandible (Fig. 3a). The dorsal extremity of the neural spine is preserved on an adjacent block. The axis is partially obscured by the overlying left atlantal neural arch and quadratojugal: the anterior part of the neural arch, prezygapophyses and centrum are not visible. The neural arch consists of a stout, robust pedicle and a neural spine that is anteroposteriorly expanded and arched dorsally, forming a broad, fan-like plate in lateral view. The lateral surface of the neural spine is flat, but it supports a short, blunt-ended,

finger-like transverse process (Fig. 3a: axtp) that extends ventrally and slightly posteriorly from a point level with the junction between the neural arch pedicle and spine. The distal end of this process would have formed the diapophysis for the axial rib – this articular surface is obscured by the quadratojugal. Anteriorly, the base of this transverse process is supported by a low anteroposteriorly extending ridge that may have connected anteriorly to the posterior margin of the prezygapophysis, as occurs in *Dollodon bampingi* (Norman 1986, fig. 25). Posteriorly, the neural spine bifurcates in dorsal view to form two posterolaterally directed buttresses. These buttresses are strongly expanded transversely with respect to the neural spine and each bears a large, ventrally directed and elliptical postzygapophyseal facet (Fig. 3a: axpoz). In posterior view, the buttresses narrow in transverse width above the postzygapophyseal facets, before expanding again to form the epipophyses (Fig. 3a: axepi). The latter are not as transversely wide as the postzygapophyses and do not bear obvious articular facets, but end in bluntly rounded apices. In lateral view, the postzygapophyses extend farther posteriorly than the dorsoventrally projecting epipophyses, and a shallow anteriorly extending concavity partially separates the two structures. Similar epipophyses are present anterodorsal to the postzygapophyses in other non-hadrosaurid iguanodontians, including *Iguanodon bernissartensis* (Norman 1980, fig. 24) and *Dollodon bampingi* (Norman 1986, fig. 25).

As with the atlas, the incomplete exposure of the axis limits comparisons to other non-hadrosaurid iguanodontians. Moreover, the morphology of the axis has been documented in only a handful of taxa. In *Jinzhousaurus*, the dorsal margin of the epipophysis is positioned ventral to the dorsal margin of the neural spine and the neural spine is broad and fan-shaped, with a strongly convex dorsal margin. A similar condition also occurs in *Iguanodon bernissartensis* (Norman 1980, fig. 24). By contrast, in *Dollodon bampingi* (Norman 1986, fig. 25) and *Ouranosaurus nigeriensis* (Taquet 1976, fig. 37), the dorsal margin of the epipophysis is positioned at the same level as the dorsal margin of the spine; moreover, the dorsal margin of the spine is only slightly convex in *Dollodon bampingi* and flat in *Ouranosaurus*. The neural spine of the atlas of *Camptosaurus* spp. differs significantly from that of *Jinzhousaurus* in being low and elongated anteroposteriorly, with a concave dorsal margin (Carpenter & Wilson 2008, fig. 6).

2.2.3. Postaxial cervical vertebrae. Eight of the cervicals (4–11) form an articulated series, of which cervicals 4–7 and a small fragment of cervical 8 are on the skull block (Fig. 2a), while the remainder of cervical 8 and cervicals 9–11 are preserved on the anterior of the two postcranial blocks. One cervical vertebra (cervical 3) is disarticulated (Fig. 3a: cv3), is visible in ventral view adjacent to the ventral margin of cervical 4, and has been strongly compressed dorsoventrally such that its lateral surfaces are exposed. The remaining cervicals are exposed in left ventrolateral view, with small portions of the right lateral surfaces of the centrum exposed by crushing in the anterior part of the column. Some details are further obscured by the presence of overlying cervical ribs and other elements and the tight articulation of the vertebrae. The cervicodorsal junction is unclear, as the vertebrae in this area are not fully exposed and the relative positions of the parapophyses cannot be determined. Therefore, it has been assumed there are eleven cervical vertebrae, as occurs in *Dollodon bampingi*, *Iguanodon bernissartensis*, *Mantellisaurus atherfieldensis*, and *Tethyshadros insularis* (Hooley 1925; Norman 1980, 1986; Dalla Vecchia 2009). However, this cannot be confirmed beyond doubt on the basis of the available material, especially as the last cervical and first dorsal are often highly similar in non-hadrosaurid iguanodontians (e.g., Norman 1986, figs 26, 29; Norman 2002, fig. 17).

The cervical centra are opisthocoelous, as is typical of non-hadrosaurid iguanodontians (Norman 1980, 1986; Weishampel *et al.* 2003), with a well developed anterior convexity and posterior concavity (visible on all cervicals, though largely obscured due to the close articulations of adjacent centra). In lateral view, the main bodies of the centra are almost square in outline, although the posterior margins of the cervical centra are slightly taller dorsoventrally than are the anterior margins. A shallow depression covers the anterior part of the lateral surface. This depression shallows posteriorly so that the posterior part of the lateral surface is more planar. There is a well developed rim marking the anterior, dorsal and ventral margins of the depression. A large nutrient foramen is present in the centre of the lateral depression (Fig. 3a: for): this foramen is generally subcircular in outline, but is larger and subtriangular in cervical 5. In cervicals 6–7, a second smaller circular foramen is present, situated posterodorsal to the main foramen.

The parapophysis is present as a depression on the anterodorsal corner of the lateral surface of each centrum (Fig. 3a: pa). It has an elliptical outline with the long axis of the ellipse extending anteroposteriorly, is well defined by a distinct lip or rim of raised bone, and faces either dorsolaterally (cervical 4) or mainly laterally (more posterior cervicals). The parapophysis is smallest in cervical 4 and increases in anteroposterior length posteriorly.

In ventral view, the centra are hour-glass shaped due to the contraction of both lateral margins at approximately midlength. A prominent rugose keel extends along the entire length of the ventral midline (Fig. 3a: vk): this keel is transversely flat and gently arched dorsally along its length.

Most details of the neural arches and spines are obscured by the presence of cervical ribs and/or matrix. However, where visible, the arches are indistinguishably fused to the centra. The neural arch pedicles do not extend for the entire length of the centrum, but terminate at a short distance from both its anterior and posterior margins. The pedicle is a short, robust and vertically orientated pillar of bone. The diapophyses (visible for cervicals 5–11) are positioned at the end of short, square-ended, finger-like transverse processes (Fig. 3a: dia), the tip of which is slightly expanded dorsoventrally relative to its shaft. These transverse processes extend either posterolaterally (cervical 5) or dorsolaterally (cervicals 6–11) from the neural arch. The transverse processes become increasingly elongated in the posterior part of the neck (cervicals 8–11). The prezygapophyses (the left prezygapophysis of cervical 4 is the only one exposed; Fig. 3a: cvprz) extend anterodorsally from the neural arch, forming an angle of approximately 40 degrees with the dorsal margin of the centrum. No other details of the neural arch can be determined.

The incomplete exposure of the postaxial cervicals again limits comparisons; they appear to be very similar in nearly all aspects of their anatomy to the cervicals of other non-hadrosaurid iguanodontians (e.g., *Camptosaurus aphanoecetes*, Carpenter & Wilson 2008, fig. 6; *Dollodon bampingi*, Norman 1986, fig. 26; *Iguanodon bernissartensis*, Norman 1980, fig. 22; *Mantellisaurus atherfieldensis*, Hooley 1925, fig. 5; *Ouranosaurus nigeriensis*, Taquet 1976, fig. 38). One notable difference is that the nutrient foramina are positioned relatively more posteriorly on the centrum in *Iguanodon bernissartensis* and *Mantellisaurus atherfieldensis*, and a second smaller foramen has not been reported (Hooley 1925; Norman 1980). Multiple nutrient foramina are present in the cervicals of '*Probactrosaurus*' *mazongshanensis* (Lü 1997).

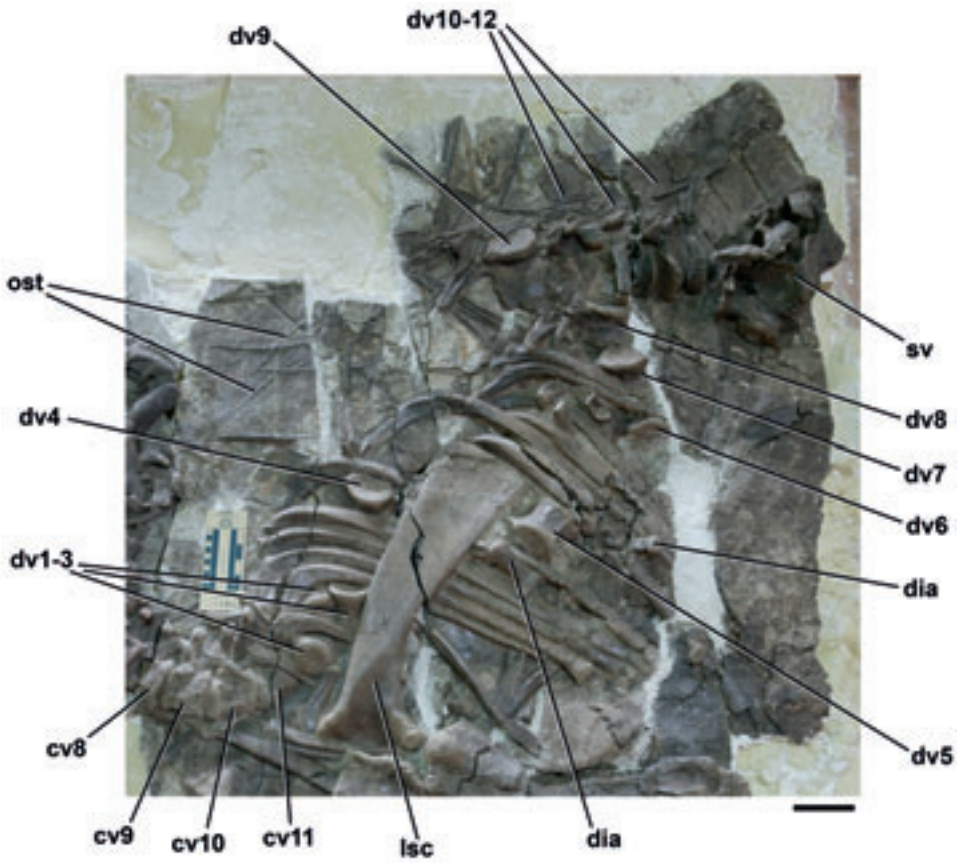

Figure 4 *Jinzhousaurus yangi*, IVPP V12691 (holotype): posterior cervical, dorsal and sacral vertebrae, ribs, left scapula. Abbreviations: cv8–cv11=cervical vertebrae; dia=diapophysis; dv1–dv12=dorsal vertebrae; lsc=left scapula; ost=ossified tendons; sv=sacral vertebrae. Scale bar=10 cm.

2.2.4. Cervical ribs. Cervical ribs are preserved alongside the articulated cervical series (Fig. 3a, cvrb); they become progressively longer posteriorly within the series. In general, the ribs are relatively short and do not extend for more than the length of a single cervical centrum. All of the ribs appear to be bicephalous, although some of the heads of the anteriorly situated ribs are narrower and partially obscured by matrix: these may only have been single-headed.

The proximal portion of the rib is transversely expanded to form a plate of bone subdivided into the capitulum and tuberculum. The latter processes extend at approximately 90 degrees to each other. In most cases, the capitulum is either broken or partially obscured, but where fully exposed it is a long slender process that ends in a rounded apex anteriorly. The tuberculum has a broader base than the capitulum, but the former is a much shorter and stouter process than the latter. The shaft tapers posteriorly to an acute tip. Its lateral surface is gently convex to planar along its length. In medial view, a strong ridge extends along the entire length of the cervical rib from the dorsomedial corner of the capitulum in a straight line along the shaft. This ridge results in the shaft having a sub-triangular transverse cross-section.

2.2.5. Dorsal vertebrae. At least 12 dorsal vertebrae are preserved, on the basis of the number of exposed centra (Figs 2, 3b, 4). Few details of individual dorsal vertebrae can be determined due to their orientation in the slab, or the presence of overlying elements (pectoral girdle, dorsal ribs). In the following description and in the table of measurements, dorsal vertebrae are numbered sequentially (in inverted commas) from anterior to posterior as preserved on the bedding plane; however, these numbers do not necessarily correspond to the position of individual vertebrae within the complete vertebral series.

The dorsal series is generally disarticulated. Dorsals '10–12' appear to represent an articulated series. Dorsals '6–8' are closely associated but not articulated. The morphology of dorsal '9' suggests that dorsals '6–12' in total represent a partially complete series. Dorsals '1–5' are not in articulation, and it is likely that several vertebrae are missing from the central part of the dorsal column – these may be present within the slabs but obscured by the presence of overlying elements. At least two diapophyses emerging from the slab in the region of dorsals '5' and '6' may represent some of these missing vertebrae (Fig. 4: dia). As far as can be determined, none of the dorsal centra possess on their lateral surfaces the large foramina seen in the cervicals, although much smaller foramina are sometimes present (e.g., dorsal '5'). Neural arches and centra are indistinguishably fused where visible.

A group of three dorsal centra (dorsals '1–3') are closely associated with the base of the neck but are not articulated with one another (Fig. 4: dv1–3). It is likely that a neural spine and diapophysis in this area pertain to one of these centra, but the correct associations cannot be determined. The anteriormost centrum has a mildly convex anterior articular surface, with a heart-shaped outline transversely wider than dorsoventrally deep. This centrum lacks a ventral keel; instead, the ventral margin of the centrum bears a longitudinal groove bounded by low longitudinal ridges. The lateral surfaces of the centrum are strongly concave; no other details can be determined. The next dorsal centrum in the series is only partially visible and has a slightly concave articular surface; however, it cannot be determined whether this is the anterior or the posterior articulation. The final centrum in this group is visible only in ventral view: it lacks both a keel and a groove and has a concave posterior articular surface. As with the first centrum, the lateral surface of the centrum is strongly concave.

A dorsal vertebra with an articulated neural arch and spine represents the next in the series (dorsal '4'; Fig. 4: dv4), lying anterior to the dorsal margin of the scapula as preserved. It is visible in posterior view only and is partially occluded by a dorsal rib. The ventral surface of the centrum possesses a low longitudinal keel. The posterior articular surface is concave and its transverse width exceeds its dorsoventral height. The neural spine is a simple, anteroposteriorly short, transversely compressed plate of bone broken at its dorsal margin. At the base of the neural spine, the two postzygapophyses flare outwards and have sub-ovate articular facets that are directed ventrolaterally. A shallow sulcus separates the two postzygapophyses posteriorly.

The next dorsal centrum (dorsal '5') is situated posterior to the ventral margin of the scapula (Fig. 4: dv5). It is amphiplatyan with a keeled ventral surface. The lateral surface is separated into two distinct concavities, one facing ventrolaterally and the other laterally, separated by a distinct, longitudinal break in slope. A neural arch is associated with this vertebra, but is covered by the scapula. The anterior articular surface is shield-shaped, with a dorsoventral height that exceeds its transverse width.

Dorsal '6' is visible in left lateral view, but a rib fragment largely obscures the vertebra and the transverse process is broken (Fig. 4: dv6). The anterior articular surface is flat to gently concave. The neural arch pedicle is stout and gives rise to the prezygapophyses anteriorly. The left prezygapophysis appears to be broken at its tip and forms a stout subtriangular process in lateral view. The parapophysis has migrated onto the neural arch (this is probably also the case in the preceding dorsals, but the parapophysis is not exposed) and forms a large subcircular facet on the lateral surface of the arch, between the diapophysis and the base of the prezygapophysis. The lateral surface of the parapophysis is concave and surrounded by a distinct rim of bone. The transverse process extends dorsolaterally and bears a ridge on its ventral surface that gives the process a subtriangular cross-section: this ridge is bounded anteriorly by a shallow groove. A similar ventral ridge is present in *Iguanodon bernissartensis* (Norman 1980, fig. 37).

Dorsal '7' is visible in posterolateral view, and includes a centrum and neural arch, most of which is obscured by overlying ribs (Fig. 4: dv7). As far as can be determined, the centrum is almost identical to that of dorsals '5' and '6'. The posterior articular surface is gently concave and has a shield-shaped outline. The neural canal is small and circular in outline. The transverse process extends dorsolaterally and bears a central ridge on its ventral surface with a groove posterior to it. The dorsal termination of the transverse process is slightly expanded to form the blunt diapophysis. The postzygapophyses are subtriangular flanges that extend beyond the posterior margin of the centrum; each postzygapophysis bears a large elliptical ventrolaterally facing articular facet.

Dorsals '8' and '9' are visible in posterolateral and posterior views respectively, and are essentially identical to dorsal '7' (Fig. 4: dv8, dv9). Dorsals '10' and '11' are preserved in left lateral view (Figs 3b, 4: dv11, dv10–12), although dorsal '11' is broken, as it was split between two slabs during collection. Both vertebrae are obscured by matrix, ribs and overlying ossified tendons; as far as can be determined the two vertebrae are highly similar in morphology. The following description is based upon dorsal '10'. The prezygapophysis extends anterior to the anterior margin of the centrum; it has a large elliptical dorsomedially facing facet. The dorsal margin of the prezygapophysis merges with the base of the transverse process in lateral view. The transverse process is broken, and has an elliptical cross-section with the long axis of the ellipse oriented anteroposteriorly. Unlike in preceding dorsals where the transverse processes project dorsolaterally, the transverse processes of dorsals '10' and '11' project mainly laterally. There is no evidence of a separate parapophysis, suggesting that it may have merged with the base of the diapophysis, as occurs in posterior dorsals of *Dollodon bampingi* (Norman 1986, fig. 31) and *Iguanodon bernissartensis* (Norman 1980, fig. 37). A broad rounded ridge is present on the posteroventral margin of the transverse process. The neural spine is an anteroposteriorly expanded and transversely flattened plate of bone and is associated with an in situ set of ossified tendons.

Dorsal '12' is complete and visible in left lateral view, although postzygapophyses are not exposed (Figs 3b, 4: dv12, dv10–12). The anterior articular surface is gently concave while the posterior surface is strongly concave, although this concavity may have been accentuated by distortion. The ventral surface of the centrum is gently rounded, lacking a midline groove or keel, and merges smoothly into the concave lateral surfaces of the element. The neural arch pedicle is limited to the anterior half of the centrum. The prezygapophyses are stout subtriangular processes in lateral view, with dorsomedially facing articular surfaces. The transverse process is broken but possessed a low rounded ridge on its ventral margin. The neural spine is an anteroposteriorly expanded and transversely flattened plate of bone.

The incomplete exposure of the dorsal vertebrae again limits comparisons; they appear to be very similar in all aspects of their anatomy to the vertebrae of other typical non-hadrosaurid iguanodontians (e.g., *Iguanodon bernissartensis*, Norman 1980, figs 34–40; *Dollodon bampingi*, Norman 1986, fig. 29–32). The dorsal series differs from that of *Ouranosaurus nigeriensis* (Taquet 1976, fig. 40) by lacking the elongated neural spines typical of that species.

2.2.6. Dorsal ribs. Remains of at least 12 left dorsal ribs and at least three right dorsal ribs (visible in medial view) are scattered through the thorax of the specimen (Figs 2, 4). Several other fragments of ribshaft are present, but cannot be assigned to a particular side of the animal. Five of the left ribs are preserved almost in articulation, and these are nearly complete. The ribs are relatively short anteriorly, reach their maximal lengths in the anterior mid-trunk region and decrease in size posteriorly (N.B., the inference that the ribs decrease in length posteriorly is based in part on a decrease in their anteroposterior width, as many of these ribs are incomplete distally). The ribs are curved in both transverse and anteroposterior planes; curvature of the ribs becomes more accentuated posteriorly as the result of greater curvature of the proximal shaft in combination with the increased length of the capitulum.

The proximal part of the rib is transversely expanded to form a plate of bone that supports the tuberculum and capitulum; these two processes are separated by a shallow notch. The capitulum is the larger of the two processes and extends almost perpendicular to the shaft of the rib, while the tuberculum forms only a very short articular process that extends in line with the rib shaft. In posterior dorsals the tuberculum becomes further reduced to a simple facet on the dorsolateral corner of the elongated capitulum. A low ridge originates from the anterolateral corner of the proximal plate, at the base of the tuberculum. This ridge extends distally along the anterolateral corner of the ribshaft. The shaft cross-section is subelliptical proximally, but becomes transversely compressed distally. Almost all of the ribshafts are broken distally; however, in one or two cases it can be seen that the distal end of the shaft is slightly expanded in an anteroposterior direction relative to the shaft. There is no evidence for any mineralised intercostal plates.

2.2.7. Sacrum. The anterior part of the sacrum, containing the sacrodorsal and sacrals 1–3 is positioned on the anterior block posterior to dorsal '12' (Figs 3b, 4). Some possible additional fragments of the sacrum, probably representing sacral ribs or neural spines, are present on the posterior block adjacent to the pubic peduncle of the left ilium, but are incompletely exposed and poorly preserved with little informative morphology. As preserved, the sacrodorsal and sacrals 1–3 are exposed in left lateral view. The sacral ribs of sacrals 1–3 are partially obscured by the transverse processes that have been crushed to their lateral surfaces. The sacrum is extensively fused: adjacent centra are fused and sutures between sacral ribs and transverse processes cannot be identified. Adjacent neural spines are not fused to one another. In all sacrals, postzygapophyses appear to be indistinguishably fused to the prezygapophyses of the succeeding vertebra. A small fragment of sacral 4 is preserved at the posterodorsal margin of sacral 3.

Part of the anterior articular surface of the dorsosacral is visible (Fig. 3b: ds), as is the left lateral surface of the centrum, the neural arch, the left prezygapophysis and part of the neural spine, although the latter is partially obscured by dorsal '12'. The articular surface is slightly convex. The lateral and ventral surfaces of the centrum are concave, with no evidence of a ventral groove or ridge. There is a stout neural arch pedicle and a sub-circular neural canal. In lateral view, the prezygapophysis is a triangular flange that extends beyond the anterior face of the centrum and possesses a dorsally facing, sub-circular and flat articular surface. The transverse process is broken and there is no sign of a separate parapophysis: comparison with the dorsosacral of *Iguanodon bernissartensis* (Norman 1980, fig. 44) suggests that the parapophysis and diapophysis formed a near continuous surface.

Sacrals 1–3 (Fig. 3b) have short stout transverse processes that project horizontally, but are broken with the distal ends crushed. They have a rectangular cross-section with the long axis directed anteroposteriorly. In all cases, the lateral extremities of the transverse processes are broken. Sacral ribs are indistinguishably fused to the ventral surfaces of the transverse processes and the lateral surfaces of the neural arches and centra. In sacrals 1 and 2 the anteroposteriorly narrow, vertically oriented sacral rib is fused to the anteroventral margin of the transverse process. In sacral 3, the sacral rib is fused to the centre of the ventral margin of the transverse process. Ventrally, the sacral ribs expand anteriorly and posteriorly and join with each other to form an extensive sacral yoke that extends over most of the lateral surfaces of the sacral centra. On sacrals 1 and 2, this sacral yoke is posterodorsally directed: posterior to this it becomes more horizontal. Much of the sacral yoke of sacral 3 is damaged and missing. Few details of the sacral centra can be determined; they are incomplete and damaged ventrally and are furthermore obscured by the sacral yoke. The neural spines are anteroposteriorly expanded and transversely compressed blades that are slightly posteriorly inclined.

As with all other parts of the vertebral column, the incompleteness, and incomplete exposure, of the sacral block limits comparisons. As far as it can be compared, the sacrum appears similar to that of other non-hadrosaurid iguanodontians (e.g., *Iguanodon bernissartensis*, Norman 1980, fig. 44) although the sacral vertebrae lack the elongated neural spines seen in *Ouranosaurus nigeriensis* (Taquet 1976, fig. 40).

2.2.8. Caudal vertebrae. Thirteen caudal vertebrae are present (Fig. 5): the first seven are disarticulated; the subsequent six (caudals '8–13', as preserved) form an articulated series towards the posterior of the posterior postcranial slab. The disarticulated caudals are generally visible only in either anterior or posterior view; the articulated series is visible in left lateral view. Due to the disarticulation of the proximal caudal series, it is not possible to determine whether these vertebrae present a complete segment of the tail or if a number of caudal vertebrae are missing. There appears to be a break in the sequence between caudals '6' and '7', based upon differences in centrum size, the height of the neural spine and the extent of caudal ribs. All neural arches and caudal ribs are fused indistinguishably to their centra.

The most anterior preserved caudal vertebra (caudal '1') is positioned between the ilia (Fig 5a: cdv1). It is exposed in anterior view and its caudal ribs and neural spine are incomplete and damaged. The articular surface of the centrum is shaped like a flattened ellipse with the long axis directed transversely. It is gently concave except along its dorsal margin, where it becomes convex ventral to the neural canal. The neural canal is sub-circular. Dorsal to the neural canal, the prezygapophyses project slightly beyond the anterior surface of the centrum: they are high angled and face dorsomedially at approximately 70 degrees to the horizontal. The articular facets are sub-quadrate in outline and have a flat to slightly concave surface. Above the prezygapophyses there is an elongate, slightly posteriorly inclined and transversely compressed neural spine (Fig. 5a: ns). The caudal ribs are fused indistinguishably to the neurocentral suture and project laterally and dorsally (Fig. 5a: cdrb) and in anterior view are slightly arched along their length (they are incomplete distally). The rib has a sub-quadrangular cross-section. The lateral face of the centrum is not well exposed, but was slightly concave. There is no anterior chevron facet, suggesting that this is a very proximal caudal.

Caudal '2' is positioned between the postacetabular blades of the ilia (Fig. 5a: cdv2). It is also exposed in anterior view and is similar to caudal '1' although the ribs and spine of caudal '2' are more complete. Its anterior articular surface is not as transversely expanded as in caudal '1' and the distally tapering caudal ribs (Fig. 5a: cdrb) are more horizontally oriented (slight dorsal inflection). The caudal rib has a transverse ridge on its ventral surface that gives the base of the rib a T-shaped cross section. No obvious haemal arch facet is present.

Caudal '3' is badly eroded and is exposed posterior to the end of the postacetabular blade of the right ilium (Fig. 5b). It is exposed in anterior view, but much of the articular face of the centrum and prezygapophyses are damaged and missing. It is generally similar to preceding caudals, with the exception that its anterior articular surface is shield-shaped. There is no evidence for a haemal arch facet.

Caudal '4' is positioned posterior to the left ilium and right ischium and is exposed in left posterolateral view (Fig. 5c: cdv4). The prezygapophyses are not exposed. The posterior articular surface of the centrum is shield-shaped and strongly concave. Laterally, the surface of the centrum is concave, while the ventral surface is poorly preserved and damaged. The centum is anteroposteriorly short: its length is less than its transverse width. The caudal rib is positioned (and fused) on the neurocentral boundary and is an anteroposteriorly expanded and dorsoventrally compressed blade of bone directed laterally and slightly dorsally, arched along its length, and rounded distally (Fig. 5c: cdrb). The neural canal is a flattened ellipse in outline (Fig. 5c: nc). Above this, the postzygapophyses project beyond the posterior margin of the centrum and face ventrolaterally at an angle of approximately 70 degrees to the horizontal. Their articular surfaces are not well preserved, but appear to be flat or very gently concave. The neural spine is complete (Fig. 5c: ns), posteriorly inclined and shorter than in the earlier caudals. The caudal rib is also shorter than in caudal '2'. There is a well developed chevron

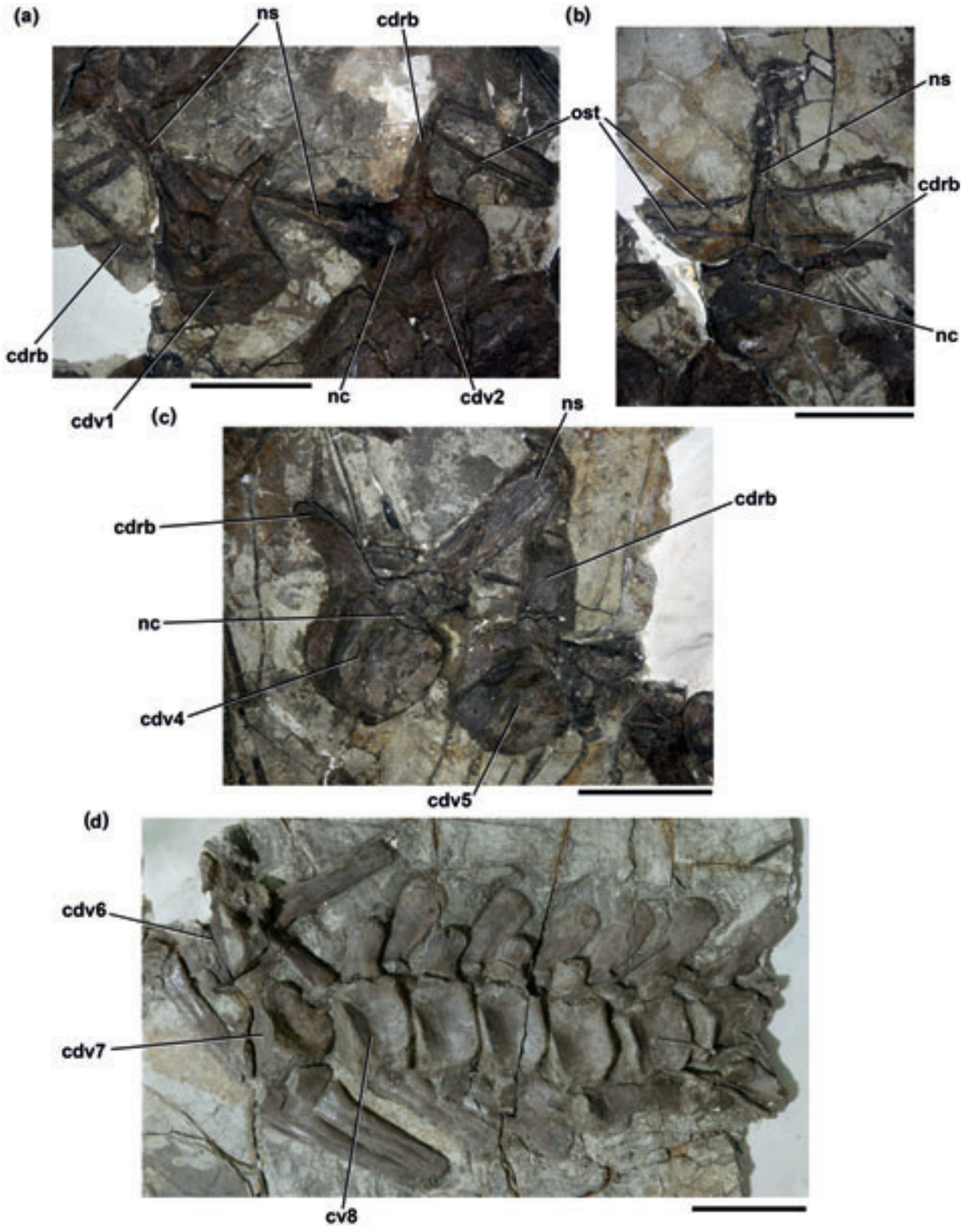

Figure 5 *Jinzhousaurus yangi*, IVPP V12691 (holotype), caudal vertebrae: (a) Caudal vertebrae '1' and '2'; (b) Caudal vertebra '3'; (c) Caudal vertebrae '4' and '5'; (d) Caudal vertebrae '6' to '13' and associated chevrons in left lateral view. Abbreviations: cdrb=caudal rib; cdv1–cdv8=caudal vertebrae; nc=neural canal; ns=neural spine; ost=ossified tendons. Scale bars=10 cm.

facet on the posterior margin of the centrum: it is concave, faces posteroventrally and is oriented at an angle of approximately 60 degrees to the horizontal. It has a flattened elliptical outline and the bone surface of the facet is more irregular and textured than the rest of the centrum surface.

Caudal '5' is exposed in left posterolateral view and is generally similar to caudal '4' (Fig. 5c: cdv5). Its neural spine is missing. The left postzygapophysis of caudal '5' is better preserved than in caudal '5': its articular surface has a subelliptical outline and is flat to slightly concave. As in caudal '4',

there is a posterior haemal arch facet, but this is damaged. There is no noticeable decrease in caudal rib length between caudals '4' and '5'. The ventral ridge is absent from the caudal rib of caudal '5'.

Caudals '6' and '7' are poorly preserved and incompletely exposed (Fig. 5d: cdv6, cdv7). In general they are similar to caudals '4' and '5', although there is a notable decrease in caudal rib length between caudals '5' and '6'.

Caudals '8–13' form an articulated series and are crushed so that the caudal ribs are visible in ventral view, partially obscuring the neural arches (Fig. 5d). In all cases this crushing has caused the caudal rib to break at its base. The anterior articular surface of caudal '8' is incompletely exposed, but is flat to very slightly concave. The height and width of the articular surface are sub-equal and are in turn sub-equal with centrum length. The lateral surface of the centrum is concave: ventrally there is a distinct break in slope that marks one of a pair of anteroposteriorly extending ridges (each ventral margin formed by a ridge), which is separated from its partner by a ventral sulcus. The caudal rib is short, anteroposteriorly broad, dorsoventrally compressed and has a rounded apex in ventral view. The zygapophyses are not well exposed, but the postzygapophysis is positioned on the neural spine at a high angle to the horizontal (although the exact angle cannot be determined). The transversely compressed neural spine is dorsoventrally short compared to that of caudals '1–6' and is only marginally longer than the depth of the centrum. It is more strongly inclined posteriorly than in caudals '1–6', is expanded in anteroposterior width dorsal to the postzygapophyses, and has a broadly rounded dorsal margin. Haemal arch facets are present both anteriorly and posteriorly. The anterior chevron facet is broad, flat to slightly convex, has a flattened elliptical outline, and is set at a low angle (20–30 degrees) to the horizontal.

Caudals '9–13' are largely similar to caudal '8'. Posteriorly, the caudal rib progressively decreases in transverse length, although it maintains a relatively constant anteroposterior length, becoming a very short process in caudal '13'. The neural spines decrease slightly in dorsoventral height along the series, but become increasingly strongly inclined posteriorly. The proportions of the centra remain similar in caudals '8–11'. In caudal '12' the centrum is slightly longer than high; in caudal '13' the length of the centrum clearly exceeds its height. Anterior and posterior haemal arch facets are present on all vertebrae, as are ventral sulci. The zygapophyses are generally poorly exposed: the prezygapophyses are set on elongate anteriorly extending pedicles and extend slightly anterior to the margin of the centrum (visible in caudals '12' and '13' only). Their articular surfaces are not preserved. The postzygapophyses are positioned on the neural arch and have a elliptical to sub-circular flat articular facet that is oriented at a high angle (70–80 degrees) to the horizontal. In caudal '12' the anterior chevron facet is strongly convex, while the posterior facet is strongly concave. In caudals '12' and '13' the anterior articular surface of the centrum is partially exposed and is concave.

As for the rest of the axial skeleton, no significant differences can be identified between the caudal vertebrae and chevrons (see below) and those of other typical non-hadrosaurid iguanodontians such as *Iguanodon bernissartensis* (Norman 1980) and *Dollodon bampingi* (Norman 1986). *Tethyshadros insularis* differs from *Jinzhousaurus* in possessing proximal caudal centra that are longer than high and low hatchet-shaped neural spines (Dalla Vecchia 2009).

2.2.9. Chevrons. Ten chevrons are preserved: the first of these is not in articulation and is situated between caudals '4' and '5' and the ischia. The second chevron is positioned close to, but not articulated with, caudal '6'. The remaining chevrons are preserved in articulation with caudals '8–13' (Fig. 5d). Chevron '1' is exposed in either anterior or posterior view: the remaining chevrons are preserved in lateral view. Chevron '1' is poorly preserved at its proximal end, but is formed by two haemal arches that join proximally to form the articular surface (so that the chevron is Y-shaped in outline). Immediately ventral to the articular facet, the haemal arches are separated by an elongate haemal canal, which has an elliptical outline. Distal to this the arches fuse to form a ventral rod that tapers in both lateral and anterior views to terminate in a rounded tip. A shallow groove extends along the midline from the ventral margin of the haemal canal terminating just above the ventral end of the chevron. Chevron '2' is very similar but slightly shorter than chevron '1': its proximal end is also damaged, but it is clearly wedge-shaped in lateral view, with a transverse ridge separating the anterior and posterior surfaces. The lateral surface of the chevron bears a centrally positioned, dorsoventrally extending and shallow groove. The chevron is not curved distally in lateral view and tapers toward its termination. Chevron '3' is associated with the anterior margin of caudal '7'. It is slightly curved along its length to project slightly posteriorly and is longer than chevron '2'. It tapers distally and lacks the groove seen on chevron '2'. Chevron '4' is associated with posterior margin of caudal '7' and is adjacent to (and slightly shorter than) chevron '3'. Chevron '4' has a lateral groove and is parallel-sided and straight (does not taper distally as occurs in the more anterior chevrons). The angle between the proximal articular facets is approximately 90 degrees. Chevrons '5–10' are closely associated with caudals '8–13', although they have moved slightly from their original positions. There is a general decrease in chevron length posteriorly. Chevrons '5' and '6' are well exposed in lateral view, but chevrons '7–10' partially overlie and obscure each other. Chevron '10' is incomplete distally. The chevrons are straight in lateral view and expand slightly (anteroposteriorly) towards their distal ends, which are broadly rounded in lateral view. A slight ridge is present on the lateral surfaces of chevron '5' and '7', but is absent from chevrons '6' and '8–10'. The surfaces of the articular facets are exposed in chevrons '8–10'. The anterior facet is slightly convex, whereas the posterior facet is concave.

2.2.10. Ossified tendons. A large number of ossified tendons are preserved, situated in the dorsal, sacral and caudal regions of the axial column (Figs 2, 4, 5: ost). As far as can be determined, no tendons are associated with the cervical series. In general, ossified tendons are isolated from the vertebral column, although they can be seen alongside the neural arches on the posterior dorsals, sacrals and caudals. The tendons are not generally preserved in the latticed arrangement present in other non-hadrosaurid iguanodontians (e.g., *Iguanodon bernissartensis*: Norman 1980; *Dollodon bampingi*: Norman 1986), although a hint of this organisation is present on dorsals '10' and '11'. The tendons are cylindrical and rod-like and their surfaces are ornamented with numerous fine, longitudinally oriented striations. The tendons range in diameter from 5–8 mm and are preserved in short sections that do not exceed 250 mm in length.

2.3. Pectoral girdle

2.3.1. Scapula. Both scapulae are present (Figs 2, 4, 6a). The left is complete and exposed in lateral view and overlies the articulated series of dorsal ribs. The right is partially exposed at its proximal end in medial view; more posteriorly it is obscured by overlying ribs, vertebrae and the left scapula. For convenience, the scapula is described with the blade oriented horizontally. The scapula consists of an elongate and transversely compressed blade and a proximal expansion that

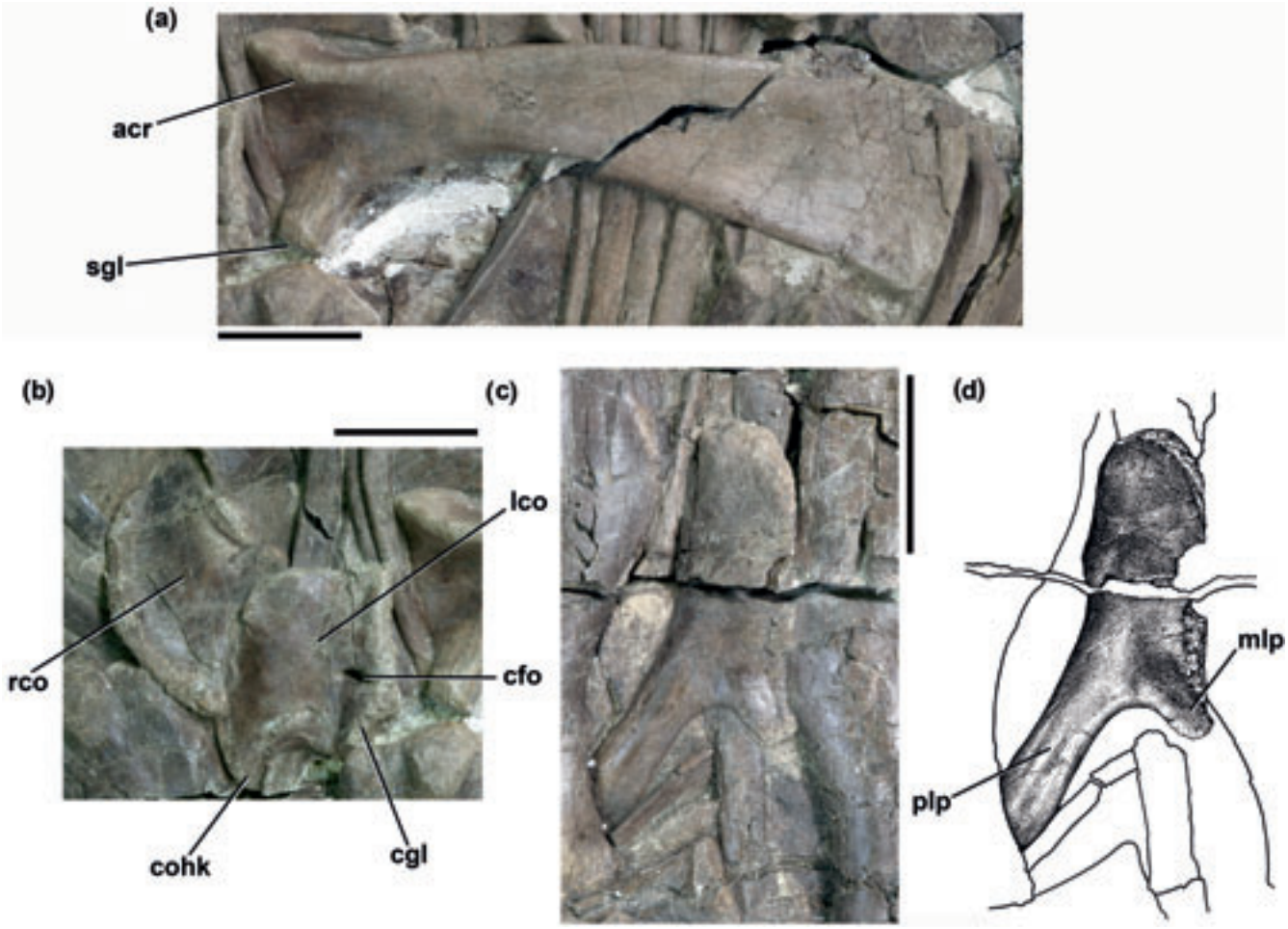

Figure 6 *Jinzhousaurus yangi*, IVPP V12691 (holotype), pectoral girdle: (a) Left scapula, lateral view; (b) Left and right coracoids, in lateral and medial views respectively; (c, d) Right sternum, external view. Abbreviations: acr=acromion process; cfo=coracoid foramen; cgl=coracoid glenoid; cohk=hook-like process of the coracoids; lco=left coracoid; mlp=midline tab-like process; plp=posterolateral handle-like process of sternum; rco=right coracoid; sgl=scapula glenoid. Scale bars=10 cm.

forms the articulation with the coracoid and that also contributes to the glenoid fossa. The blade is curved along its length in lateral view such that the dorsal margin of the blade is gently convex and the ventral margin is concave. The curvature of the ventral margin is more marked than that of the dorsal margin. As a result, towards the posterior end of the blade, the dorsal and ventral margins diverge, causing an increase in the dorsoventral depth of the blade. The dorsal margin of the blade is broadly rounded in transverse cross-section; the ventral margin is rounded anteriorly, but thins to a sharp ridge posteriorly. In dorsal view, the blade is gently bowed outward along its length to follow the contour of the rib cage. The blade becomes increasingly compressed transversely toward its posterior end, and most of the lateral surface of the blade is dorsoventrally concave. The posterior margin of the scapula is gently convex in lateral view and is smoothly finished. At the proximal end there is a small pseudoacromial process that projects anteriorly and slightly dorsally (Fig. 6a: acr). The dorsal margin of this process forms a broad, rounded ridge: posteriorly, this ridge descends posteroventrally across the scapula as a low break in slope to meet and merge with the ventral margin of the blade, dividing the scapula into anterior (the proximal plate) and posterior portions (the concave area comprising most of the blade mentioned above). Anteroventral to this ridge, the proximal plate of the scapula is covered by a deep concavity, which is deepest adjacent to the coracoid suture and decreases in prominence posteriorly. The ventrolateral margin of the anterior end of the scapula is thickened transversely to form the scapula contribution to the glenoid (Fig. 6a: sgl). This thickening has a low ridge on its posterior surface that probably served as the insertion for *M. triceps scapulare lateralis externalis* (Norman 1986). The glenoid surface is rugose and has a sub-elliptical outline, which faces anteroventrally and slightly laterally.

The articular surface for the coracoid is exposed on the left scapula and has a sub-pentagonal outline, narrowing dorsally. The articular surface is concave dorsally and has an irregular ventral surface. The ventromedial margin of the articular surface is notched to form a groove (the coracoid groove) that extends onto the anterior end of the medial surface of the scapula.

Although the morphology of the scapula is generally typical of non-hadrosaurid iguanodontians, a unique combination of features distinguishes it from the equivalent element in most other taxa. The proximal plate of the scapula is less strongly expanded than in *Iguanodon bernissartensis* (Norman 1980, fig. 52), and the blade expands in dorsoventral width toward its distal end; by contrast, the dorsal and ventral margins of the scapula blade are nearly parallel in *Iguanodon bernissartensis* (Norman 1980). Unlike the condition in *Altirhinus* (Norman 1998, fig. 25) and *Dollodon bampingi* (Norman 1986, fig. 43) the distal end of the scapula blade is neither thickened nor rugose, and there is no evidence for the presence of a cartilaginous extrascapula. The scapula of *Jinzhousaurus* lacks the 'medial buttress' described in *Camptosaurus aphanoecetes* (Carpenter & Wilson 2008, fig. 16C). Unlike the condition in

Camptosaurus dispar (Carpenter & Wilson 2008, fig. 17), *Mantellisaurus atherfieldensis* (Hooley 1925, fig. 7) and *Probactrosaurus gobiensis* (Norman 2002, fig. 20) the blade of the scapula of *Jinzhousaurus* is curved along its length in lateral view. The scapula of '*Probactrosaurus*' *mazongshanensis* (Lü 1997, fig. 9) differs from that of *Jinzhousaurus* in that the dorsal margin of the blade is straight (rather than curved) and the distal end of the blade is strongly convex in lateral view. The scapula of *Tethyshadros insularis* (Dalla Vecchia 2009, fig, 5A) differs from that of *Jinzhousaurus* in being more strongly and asymmetrically expanded at its distal end. The scapula is either unknown or undescribed in other non-hadrosaurid iguanodontians.

2.3.2. Coracoid. Both coracoids are present (Figs 2, 6b). The left coracoid is visible in lateral view whereas the right coracoid is visible in medial view. The coracoids are not fused to the scapulae. In lateral view, the coracoids are subquadrate plates with an almost straight dorsal margin, a vertically inclined and gently curved anterior margin, a short and strongly curved ventral margin, and a subvertical posterior margin divided into the facet for the scapula and the coracoid contribution to the glenoid fossa. The anterior margin of the coracoid curves medially to form a vertically inclined articular surface; this surface is strongly rugose and would have articulated with the sternum (via cartilage, see Norman 1980, fig. 56). The medial surface of the coracoid is generally gently concave, although it becomes convex in the region of the coracoid foramen. The dorsal half of the lateral surface of the coracoid is gently concave, the central portion is flat to gently convex, while ventrally the lateral surface is thickened, strongly convex dorsoventrally and concave anteroposteriorly (the latter reflecting the ventral curvature). The anterior part of the lateral surface is flat, but is bevelled medially with respect to the rest of the lateral surface. A large elliptical coracoid foramen is positioned adjacent to the scapular articulation but fully enclosed within the coracoids (Fig. 6b: cfo), with the long axis of the foramen oriented anteroposteriorly. On the medial surface of the coracoid this foramen leads into a shallow anteroposteriorly extending groove that would have communicated with the coracoid groove on the scapula. In posterior view, the scapula articulation is subtriangular in outline, and widened ventrally toward the glenoid. It is separated from the glenoid by a transverse ridge. The glenoid faces posteroventrally, is rugose and has a subquadrate outline (Fig. 6b: cgl). In lateral view the anteroventral corner of the coracoid forms a small hook-like process (Fig. 6a: cohk).

The coracoid of *Jinzhousaurus* generally resembles the equivalent element in other non-hadrosaurid iguanodontians (e.g., *Dollodon bampingi*, Norman 1986, fig. 44; *Mantellisaurus atherfieldensis*, Hooley 1925, fig. 7; *Ouranosaurus nigeriensis*, Taquet 1976, fig. 48). However, it differs from the condition in *Camptosaurus* (Gilmore 1909, figs 24, 40; Carpenter & Wilson 2008, figs 16, 17) in possessing a more strongly developed hook-like process in the anteroventral corner of the element. It can also be distinguished from *Iguanodon bernissartensis*: the coracoid foramen of the latter forms a notch in the posterior margin of the element, rather than a fully enclosed foramen as in *Jinzhousaurus*. Both *Altirhinus kurzanovi* (Norman 1998, fig. 26, 'ri') and *Probactrosaurus gobiensis* (Norman 2002, fig. 20, 'ri') possess a nearly vertical ridge on the anterodorsal corner of the lateral surface of the coracoid; in *Jinzhousaurus* there is a break in slope that begins in a similar position (the anterodorsal corner of the element) but this extends posteroventrally, rather than ventrally, across the element and is less pronounced than in either of the former taxa. The coracoid is either unknown or undescribed in other non-hadrosaurid iguanodontians.

2.3.3. Sternal. The right sternal is preserved in external view (Fig. 6c, d) and is hatchet-shaped, as is generally the case among ankylopollexian iguanodontians. The main body of the sternal is subrectangular and tapers slightly in transverse width posteriorly. The anteromedial corner is thickened and rugose, marking the attachment of the element to a coracosternal cartilage. A prominent process (the handle of the hatchet) arises from the posterolateral corner of the sternal (Fig. 6c, d: plp): this process is elongate and strap-like, with subparallel sides. The medial margin of the main body is partially obscured by the left humerus and has been damaged. The lateral margin of the main body describes a smooth curve as it merges into the posterolateral process. Posteriorly, the posterolateral process is separated from a tab-like, midline extension of the main body (Fig. 6c: mlp) by an angle of approximately 80 degrees. The external surface of the sternal is gently convex transversely and longitudinally.

A hatchet-shaped sternal similar to that seen in *Jinzhousaurus* is found in many ankylopollexians (e.g., *Iguanodon bernissartensis*, Norman 1980, fig. 54; *Dollodon bampingi*, Norman 1986, fig. 45; *Mantellisaurus atherfieldensis*, Hooley 1925, fig. 7), but is absent in non-iguanodontian ornithopods (e.g., Galton 1974) and in basal iguanodontians including *Camptosaurus* (Carpenter & Wilson 2008, fig. 18). However, the sternal of *Jinzhousaurus* can be distinguished from those of all other non-hadrosaurid iguanodontians by the presence of the aforementioned tab-like midline process. *Altirhinus kurzanovi* (Norman 1998, fig. 26), *Fukuisaurus tetoriensis* (Kobayashi & Azuma 2003, fig. 5E), *Iguanodon bernissartensis* (Norman 1980, fig. 54), *Lanzhousaurus magnidens* (You *et al.* 2005, fig. 3B), *Lurdusaurus arenatus* (Taquet & Russell 1999, pl. 2.1), *Mantellisaurus atherfieldensis* (Hooley 1925, fig. 7), *Ouranosaurus nigeriensis* (Taquet 1976, fig. 49) and *Probactrosaurus gobiensis* (Norman 2002, fig. 21) all lack this structure. A short midline extension is present in *Dollodon bampingi* (Norman 1986, fig. 45), but is much less well developed than in *Jinzhousaurus*. Sterna are unknown in other non-hadrosaurid iguanodontians. The unique morphology of the sternal is proposed as an autapomorphy of *Jinzhousaurus*.

2.4. Forelimb

Both forelimbs are present and articulated (Figs 2, 7). The left forelimb is well exposed in lateral view, although the radius appears to have shifted distally relative to the ulna, and the distal end of the ulna is broken. The right ulna and radius lie beneath those of the left side and only their proximal ends are visible. The surfaces of the left radius and ulna are extensively fractured.

2.4.1. Humerus. Both humeri are present and exposed in posterior view (Figs 2, 7a). The humerus is ~67% the length of the femur. The humerus is a sigmoidal element with proximal and distal transverse expansions connected by a shaft. The transverse width of the broad and anteroposteriorly flattened proximal expansion exceeds that of the distal expansion. The head is positioned on the centre of the posterior margin of the proximal end and is a large and prominent spherical structure that projects posterodorsally (Fig. 7a: hh). A broad rounded eminence on the posterior surface of the bone supports the head ventrally; this eminence extends distally along the shaft, merging with the shaft at approximately 50% humeral length. On either side, the head is supported by the medial and lateral tuberosities. The proximal surface of the head and tuberosities is strongly rugose. The lateral margin of the proximal shaft is folded to project anteriorly, forming the margin of the deltopectoral crest (Fig. 7a: dpc). The deltopectoral crest is poorly exposed. There is a prominent roughened area on the posterolateral margin of the deltopectoral crest (right humerus) that

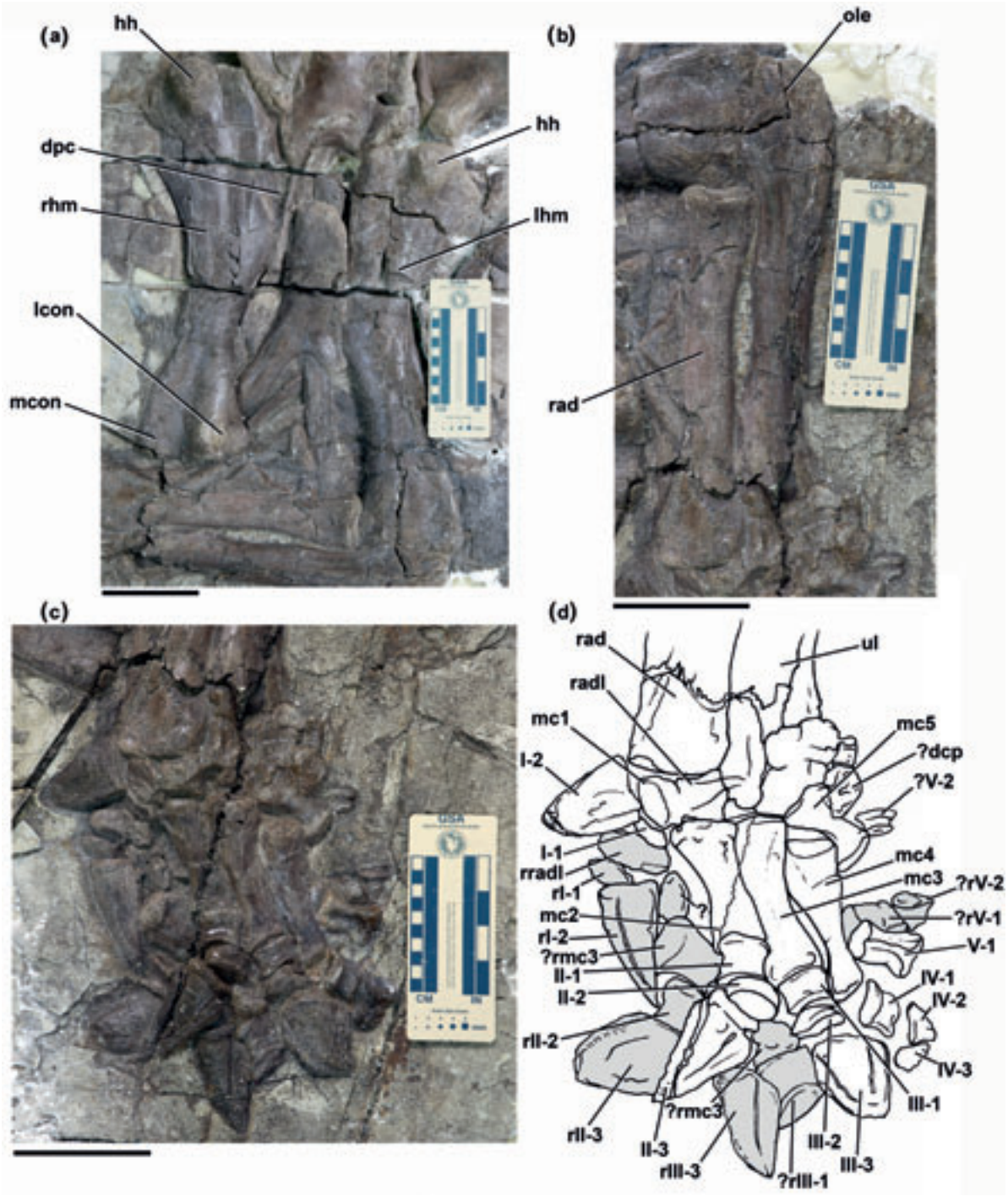

Figure 7 *Jinzhousaurus yangi*, IVPP V12691 (holotype), forelimb: (a) Humeri, right sternum, and left ulna and radius; (b) Left ulna and radius; (c) Left and right manus; (d) Interpretive drawing of the left and right manus. Elements filled grey are identified as being from the right manus (the prefix 'r' indicates that an element is identified as from the right hand). Abbreviations: I-1, I-2, II-1–V-2=manual phalanges; dcp=distal carpal; dpc=deltopectoral crest; hh=head of humerus; lcon=lateral condyle; lhm=left humerus; mc1–mc5=metacarpals; mcon=medial condyle; ole=olecranon process of ulna; rad=radius; radl=radiale; rhm=right humerus; ul=ulna. Scale bars=10 cm.

probably represents a muscle scar for the insertion of *M. deltoides-clavicularis* (Norman 1986). At its midlength, the cross-section of the shaft is a flattened ellipse, with the long axis oriented transversely. Distally, the lateral condyle (Fig. 7a: lcon) is broader in posterior view than the medial condyle (Fig. 7a: mcon).The lateral and medial condyles are separated by a deep olecranon fossa on the posteroventral surface of the humerus; the articular surfaces of the condyles are not exposed.

The morphology of the humerus is extremely similar to that seen in a number of other non-hadrosaurid iguanodontians, particularly *Altirhinus kurzanovi* (Norman 1998, fig. 27), *Camptosaurus* (Gilmore 1909, fig. 25), and *Mantellisaurus atherfieldensis* (Hooley 1925, fig. 7), which share with *Jinzhousaurus* a similar sigmoidal morphology and the enlarged and spherical head positioned on the posterior surface (the latter feature is a synapomorphy of Iguanodontia: Norman 1998). The humerus of *Dollodon bampingi* is generally similar to that

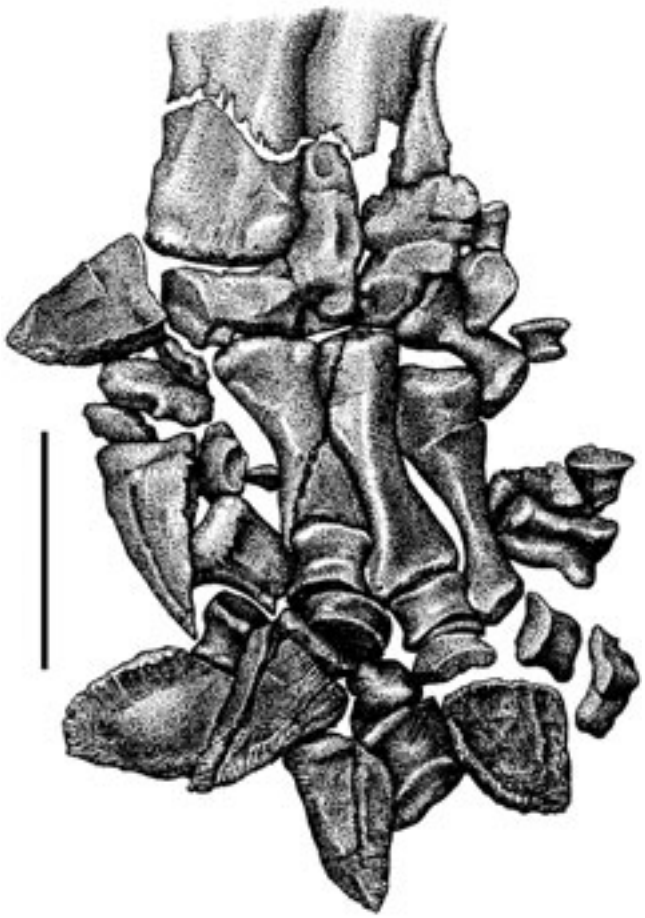

Figure 8 *Jinzhousaurus yangi*, IVPP V12691 (holotype), left and right manus (see Fig. 7 for labels). Scale bar = 10 cm.

of *Jinzhousaurus*, but is more strongly bowed laterally at its proximal end (Norman 1986, fig. 47). The humerus is short relative to the femur in both *Dollodon bampingi* (humerus is 58% femoral length; Norman 1986) and *Mantellisaurus atherfieldensis* (humerus is 56% femoral length; Hooley 1925) compared to that of *Jinzhousaurus*. However, the humerus of *Iguanodon bernissartensis* (Norman 1980, fig. 57) differs from that of *Jinzhousaurus* in that the proximal end is less strongly expanded transversely relative to the width of the shaft. Moreover, the lateral margin of the shaft between the lateral tuberosity and the apex of the deltopectoral crest is concave in posterior view in *Iguanodon bernissartensis*, rather than gently convex as occurs in *Jinzhousaurus*. In addition, the humerus of *Iguanodon bernissartensis* is elongated relative to the femur (humerus is 77–80% femoral length; Norman 1986) compared with the proportions seen in *Jinzhousaurus*. The humerus of *Probactrosaurus gobiensis* (Norman 2002, fig. 22) is similar to that of *Iguanodon bernissartensis*: in these taxa the humeral shaft is only slightly expanded transversely at its proximal end, in contrast to the condition present in *Jinzhousaurus*. The humerus of *Ouranosaurus nigeriensis* (Taquet 1976, fig. 50) differs from that of *Jinzhousaurus* in having a shaft much more slender relative to its length. Furthermore, in *Ouranosaurus* the head and the medial tuberosity form a continuous surface that lacks the embayment on the posterior surface seen in *Jinzhousaurus*. In *Lurdusaurus arenatus* the apex of the deltopectoral crest is positioned distal to midshaft (Taquet & Russell 1999), thereby differing from *Jinzhousaurus*. *Nanyangosaurus zhugeii* differs from *Jinzhousaurus* in that the lateral margin of the humeral shaft between the lateral tuberosity and the apex of the deltopectoral crest is concave in anterior/posterior view and the lateral condyle extends further distally (in anterior/posterior view) than does the medial condyle (Xu *et al*. 2000, fig. 2A–C). Finally, the humerus of *Nanyangosaurus* is relatively short relative to the femur (humerus is 51% femoral length; Xu *et al*. 2000, table 2); however, it should be noted that Xu *et al*. (2000) considered their measurement for the length of the humerus questionable, as the element is not complete proximally.

The humerus of '*Probactrosaurus*' *mazongshanensis* has not been figured and was simply described as "similar to that of other iguanodontians" (Lü 1997, p. 41), while that of *Eolambia caroljonesa* has not been described or figured in sufficient detail for comparisons to be made (Kirkland 1998). Humeri are unknown in the other Asian non-hadrosaurid iguanodontians.

2.4.2. Ulna. The ulna is a columnar element (Figs 2, 7b), the proximal end of which is anteroposteriorly expanded relative to the shaft. There is a prominent olecranon process that is subtriangular in lateral view (Fig. 7b: ole). A distinct notch separates the olecranon process from the ventral part of the proximal expansion and forms the articular glenoid for the humerus. The surface of the glenoid is not exposed. The shaft has a subovate to subtriangular cross-section at midlength, as a result of a rounded ridge that extends distally along the anterior surface of the bone from just ventral to the proximal end and merges into the shaft close to its distal end. This ridge separates the anterior and lateral surfaces of the ulna, which are both gently convex transversely.

The incomplete exposure of the ulna limits both the available anatomical information and comparisons to other taxa. In general, the morphology of the ulna resembles that in other non-hadrosaurid iguanodontians (e.g., *Altirhinus kurzanovi*, Norman 1998, fig. 28; *Eolambia caroljonesa*, Kirkland 1998, fig. 9B; *Iguanodon bernissartensis*, Norman 1980, fig. 58; *Mantellisaurus atherfieldensis*, Norman 1986, fig. 49). Nevertheless, the proportions of the ulna distinguish *Jinzhousaurus* from some other non-hadrosaurid iguanodontian taxa. For example, the ulna of *Jinzhousaurus* is considerably more robust (diameter at midshaft is ~13% total length of ulna) than the ulna of *Probactrosaurus gobiensis* (diameter at midshaft is ~6% total length of ulna; Norman 2002, fig. 23) and *Nanyangosaurus zhugeii* (diameter at midshaft is ~9% total length of ulna; Xu *et al*. 2000, table 2) but less robust than the ulna of *Lurdusaurus arenatus* (diameter at midshaft is ~18% total length of ulna; Taquet & Russell 1999, pl. 3, fig. 4). The ulna is unknown in *Equijubus normani*, *Fukuisaurus tetoriensis*, *Lanzhousaurus magnidens* and '*Probactrosaurus*' *mazongshanensis*, limiting potential comparisons.

2.4.3. Radius. The radius is a columnar bone anteroposteriorly expanded at either end to form the articular surfaces (Figs 2, 7b). The proximal end is slightly asymmetrical in lateral view and extends farther anteriorly than posteriorly. The distal expansion is larger than the proximal expansion, has a depression on its anterodistal surface, and is also asymmetrical – it extends slightly farther anteriorly than posteriorly. Approximately half of the proximal articulation is exposed in dorsal view: the exposed surface is gently concave with a curved outline, suggesting that the articular surface may have had a sub-circular outline. In lateral view, the distal articular surface appears to be convex.

As for the ulna, the incomplete exposure of the radius restricts anatomical observations and comparisons. Similar morphology is present in most other non-hadrosaurid iguanodontians (e.g., *Altirhinus kurzanovi*, Norman 1998, fig. 28; *Iguanodon bernissartensis*, Norman 1980, fig. 58; *Mantellisaurus atherfieldensis*, Norman 1986, fig. 49). Similar to the ulna, the radius of *Jinzhousaurus* is more robust than that in *Probactrosaurus gobiensis* and *Nanyangosaurus zhugeii* but is

less robust than that of *Lurdusaurus arenatus* (diameter at midshaft is ~13% total length of radius in *Jinzhousaurus*; equivalent ratios are ~7% in *P. gobiensis* (Norman 2002) and *Nanyangosaurus* (Xu *et al*. 2000), and ~18% in *Lurdusaurus* (Taquet & Russell 1999)). Moreover, the proportions of the antebrachium relative to the humerus distinguish *Jinzhousaurus* from several other non-hadrosaurid iguanodontians for which measurements are available. In *Jinzhousaurus*, the radius is ~63% the length of the humerus; the equivalent ratio is ~55% in *Lurdusaurus* (Taquet & Russell 1999, table 2), ~71% in *Mantellisaurus atherfieldensis* (Hooley 1925), ~75% in *Ouranosaurus nigeriensis* (Taquet 1976), ~80% in *Dollodon bampingi* (Norman 1986, appendix 2), 87% in *Nanyangosaurus zhugeii* (Xu *et al*. 2000; however, as noted above, Xu *et al*. (2000) considered their humeral length measurement questionable), and 98% in *Tethyshadros insularis* (Dalla Vecchia 2009). The radius of *Iguanodon bernissartensis* is similar in relative length to that of *Jinzhousaurus*: it is ~60–67% the length of the humerus. Radius/humerus ratios are unavailable for *Altirhinus* and *Probactrosaurus gobiensis* (Norman 1998, 2002) and the radius is unknown in other Asian taxa.

2.4.4. Manus. Both hands are preserved (Figs 2, 7c, d, 8), with the left hand directly superimposed over the right, largely obscuring it. In the following description (most of which is based upon the left manus) the hand is described as if held horizontally, with the palm facing downward. The left hand is visible mainly in dorsal view and appears to be almost complete (Fig. 7c, d), with the exception of digits IV and digit V, both of which may be missing distal phalanges. Both hands are preserved in a supinated position. The elements of the left hand are mainly articulated, but one or two small elements lie outside of their life positions. The carpus is poorly preserved. It is possible that many of the elements have fused, as also occurs in *Iguanodon bernissartensis* (Norman 1980) and (to a lesser extent) *Mantellisaurus atherfieldensis* (Norman 1986, fig. 50), as sutures are difficult to determine. Nevertheless, differences in bone texture, and grooves between these elements, do allow the recognition of some separate elements.

Metacarpal I is incorporated into the carpus (Fig. 7c, d: mc1): it appears to be fused with the radiale laterally, but can be distinguished from it by a shallow groove. It has an irregular pentagonal outline in dorsal view, and its dorsal surface is saddle-shaped. It articulates with the distal end of the radius. The radiale is a rectangular element with a convex dorsal surface that also articulates with the distal end of the radius (Fig. 7c, d: radl). Lateral to the radiale are several large bone elements that cannot be positively identified. It is likely that some of these elements represent the intermedium, ulnare and the distal carpals, but the poor preservation of these elements precludes further identification. Metacarpals II–III are closely appressed to one another and are only visible in dorsal view (Fig. 7c, d: mc2, mc3, mc4). Metacarpal III is the longest in the hand, followed by metacarpal IV and then metacarpal II. Metacarpal II is an elongate rod-like element that possesses a straight shaft with a subcylindrical cross-section. Its articular surfaces are obscured, but they appear to be transversely expanded with respect to the shaft. Metacarpal III also has articular surfaces that are transversely expanded relative to the shaft – this expansion is more marked than in metacarpal II. The shaft of metacarpal III is straight, and may have had a subquadrangular cross-section. The dorsal surface is gently concave along its length and is separated from the medial surface by a distinct break-in-slope. There is no evidence for a collateral ligament pit on the medial surface of the distal end. Metacarpal IV is visible in dorsomedial view. As with the other metacarpals it is columnar with expanded proximal and distal ends. The proximal articulation has a subovate outline. The medial surface of metacarpal IV is grooved for the reception of metacarpal III. Metacarpal V is a small dumbbell-shaped bone (Fig. 7c, d: mc5) with a dorsal surface that is strongly convex transversely, and strongly concave proximodistally. The distal articular surface is rounded and has a subtriangular outline.

A small strap-like element that lies immediately distal to metacarpal I probably represents phalanx I-1 (Fig. 7c, d: I-1). Phalanx I-2 is a triangular thumb-spike with a dorsal surface that is gently convex both proximodistally and mediolaterally (Fig. 7c, d: I-2). The distal end of the element is incompletely exposed. Digit II bears three phalanges, inclusive of a large ungual. Phalanx II-1 is a block-like element in dorsal view that is transversely wider than it is long (Fig. 7c, d: II-1). Its dorsal surface is proximodistally concave and transversely convex, producing a saddle-like surface. Phalanx II-2 is proximodistally short and subrectangular in dorsal view and it is almost three times as wide as it is long (Fig. 7c, d: II-2). Its saddle-shaped distal articular surface is partially exposed and is gently concave transversely and gently convex dorsoventrally. Ungual II-3 is large and subtriangular in dorsal view, ending in a bluntly rounded point (Fig. 7c, d: II-3). There is some evidence of longitudinal grooves along the margins of the element. Its proximal articular surface is elliptical in outline and gently concave, with the long-axis of the ellipse oriented transversely. In dorsal view the ungual contracts slightly transversely distal to the proximal articulation, before expanding outward again to form the main body of the ungual. Phalanges III-1 and III-2 are essentially identical to those of the second digit, but are slightly shorter proximodistally (Fig. 7c, d: III-1, III-2). Ungual III-3 is very similar to that of the second digit, although it appears to be slightly broader, giving it a more hoof-like outline (Fig. 7c, d: III-3). It is damaged at its distal margin. Three phalanges appear to be associated with digit IV. Phalanx IV-1 is essentially similar to phalanges II-1 and III-1 (Fig. 7c, d: IV-1). Two small poorly preserved bones positioned distal to this probably represent IV-2 and IV-3 (Fig. 7c, d: IV-2, IV-3). Collateral ligament pits are not observed on any of the phalanges, nor are there any dorsal lappets.

A cluster of small phalanges lateral to digit IV represents parts of left and right digits V, which have become disarticulated. Phalanx V-1 is the largest non-ungual phalanx in the hand. It is a subrectangular element in ventral view with expanded proximal and distal articulations and a gently concave ventral surface. At least one more distal phalanx appears to be present, although few anatomical details can be ascertained. The estimated phalangeal count for the manus is therefore 2–3–3–?3–?2.

Several elements of the right hand are visible in ventral view, including the fused metacarpal I and radiale, phalanx I-1, phalanx I-2 (thumb-spike), phalanx II-2, phalanx II-3 (ungual), metacarpal ?III, phalanx ?III-1, phalanx III-3 (ungual), and parts of digit V. These elements offer few anatomical details not identified in the left manus, with the exception that a longitudinal groove is present on the thumb-spike.

The metacarpus of *Jinzhousaurus* is rather broad, short and stout: the transverse width of metacarpal III at midshaft is ~25% total length, and metacarpal III is ~27% total length of the humerus. This is similar to the condition in *Iguanodon bernissartenesis* (equivalent ratios are ~22% and ~24%, Norman 1980, fig. 61; Norman 1986, appendix 2), *Camptosaurus aphanoecetes* (transverse width at midshaft is ~28% total length of metacarpal III, Carpenter & Wilson 2008, fig. 22) and *Ouranosaurus nigeriensis* (equivalent ratios are ~21% and ~20%, Taquet 1976, fig. 56), but differs from the

relatively narrow and elongate metacarpus seen in *Altirhinus kurzanovi* (transverse width of metacarpal III at midshaft is ~17% total length, Norman 1998, fig. 30), *Dollodon bampingi* (equivalent ratios are ~15% and ~35%, Norman 1986, figs 51–52, appendix 2), *Nanyangosaurus zhugeii* (equivalent ratios are ~13% and ~35%, Xu *et al*. 2000, table 2), *Probactrosaurus gobiensis* (transverse width of metacarpal III at midshaft is ~10% total length, Norman 2002, fig. 24C) and *Tethyshadros insularis* (equivalent ratios are ~10% and 46%, Dalla Vecchia 2009). In contrast, the metacarpus of *Lurdusaurus arenatus* is exceptionally robust (equivalent ratios are ~35% and ~19% Taquet & Russell 1999, pl. 3, fig. 4). The metacarpus and phalanges are unknown in *Equijubus normani*, *Eolambia caroljonesa*, *Fukuisaurus tetoriensis*, *Lanzhousaurus magnidens*, and '*Probactrosaurus*' *mazongshanensis* and the metacarpus is incomplete in the holotype specimen of *Mantellisaurus atherfieldensis* (Hooley 1925).

The manual phalanges of *Jinzhousaurus* are unusually short and broad: the most proximal phalanges of digits II–IV are all broader than long in dorsal view. Phalanx III-1 is only ~16·5% length of metacarpal III. By contrast, the proximal phalanges of digits II–IV are either subequal in breadth and length or longer than broad in *Altirhinus kurzanovi* (phalanx III-1 is ~29% length of metacarpal III; Norman 1998, fig. 30), *Dollodon bampingi* (phalanx III-1 is ~40% length of metacarpal III; Norman 1986, figs 51, 52), *Iguanodon bernissartensis* (phalanx III-1 is ~33% length of metacarpal III; Norman 1980, fig. 61), *Lurdusaurus arenatus* (Taquet & Russell 1999, pl. 3, fig. 4), *Mantellisaurus atherfieldensis* (Hooley 1925, fig. 8), *Nanyangosaurus zhugeii* (phalanx III-1 is ~24% length of metacarpal III; Xu *et al*. 2000, fig. 2E), *Ouranosaurus nigeriensis* (phalanx III-1 is ~33% length of metacarpal III; Taquet 1976, fig. 53) and *Probactrosaurus gobiensis* (Norman 2002, fig. 25). In *Tethyshadros insularis* phalanx III-1 is also very short (14%, Dalla Vecchia 2009) relative to metacarpal III, but this is due to the extreme elongation of the metacarpus in *Tethyshadros*, rather than reduction of the phalanges (i.e. phalanx III-1 remains longer than broad in this species). In *Camptosaurus aphanoecetes* the proximal phalanges are broader than long, but remain relatively elongate relative to metacarpal III (phalanx III-1 is ~28% length of metacarpal III; Carpenter & Wilson 2008, figs 22, 23). The presence of proximal phalanges that are both broader than long and very short relative to the metacarpus thus represents a potential autapomorphy of *Jinzhousaurus.*

The probable presence of at least three phalanges on digit IV also distinguishes *Jinzhousaurus* from *Iguanodon bernissartensis* and *Tethyshadros insularis*, in which digit IV has only two phalanges (Norman 1980; Dalla Vecchia 2009). Digit IV possesses three phalanges in *Camptosaurus* (Carpenter & Wilson 2008), *Mantellisaurus atherfieldensis* (Hooley 1925) and *Dollodon bampingi* (Norman 1986). The phalangeal count is uncertain in other non-hadrosaurid iguanodontians.

2.5. Pelvic girdle

2.5.1. Ilium. Both ilia are preserved; the left in lateral view and the right in medial view (Figs 2, 9a). The left ilium lacks the tip of the preacetabular process and several sections are missing from the dorsal part of the blade (Fig. 9a). The right ilium appears to be more complete, but its anterior extent is obscured by the left femur and ischia. The surfaces of both ilia are extensively fractured.

The elongate preacetabular process has a subovate transverse cross-section and is gently arched along its length (Fig. 9a: pre). The ventral margin of the preacetabular process is transversely thickened relative to the rest of the process, forming a ridge-like buttress that extends posteriorly and defines the ventral border of a shallow concavity on the lateral surface of the process. The ventral margin of the preacetabular process curves ventrally to merge with the anterodorsal margin of the pubic peduncle. The latter is a short, robust, anteroventrally extending process, with a subtriangular cross-section (Fig. 9a: pped). The apex of the subtriangular cross-section forms a distinct ridge that extends posterodorsally to join with the ridge-like buttress arising from the preacetabular process. Together, these ridges form a raised area that marks the anterior part of the main iliac blade. In contrast, the anterodorsal and posteroventral surfaces of the pubic peduncle are gently concave both transversely and anteroposteriorly. The posteroventral surface of the pubic peduncle forms the anterior part of the acetabular margin. A distinct break in slope, equivalent to the position of the supracetabular flange of basal ornithischians (e.g., Butler 2005), marks the dorsal boundary of the acetabulum and defines the ventral margin of an extensive shallow concavity that covers most of the dorsal and central parts of the iliac blade. This concavity is continuous with that arising from the preacetabular process (see above). The dorsal margin of the ilium is transversely thickened, but it does not overhang the lateral surface of the blade to form a supraacetabular process or similar structure. Nevertheless, parts of the dorsal margin are strongly rugose, presumably for muscle attachment. The postacetabular process is an elongate and deep subtriangular lobe (Fig. 9a: poa). A broad rounded ridge extends anteroventrally from the posteroventral corner of the postacetabular process; this ridge merges with the lateral surface of the blade just dorsal to the ischial peduncle. Ventral to this ridge, the iliac blade is reflected medially to form a shallow, laterally facing, brevis fossa (Fig. 9a: brfo). The ischial peduncle is a short, transversely expanded process, the anterior margin of which merges into the acetabular margin (Fig. 9a: isped). Other details of this area are obscured by damage.

The relatively poorly preserved and exposed state of the ilia complicates comparisons to other non-hadrosaurid iguanodontians. In many ways the ilium is strikingly plesiomorphic in appearance, and highly reminiscent of the condition seen in *Camptosaurus dispar* (Carpenter & Wilson 2008, fig. 29B) with a deep body and postacetabular process and a brevis fossa visible in lateral view. The ilium can be distinguished from that of *Altirhinus kurzanovi* (Norman 1998, fig. 32), *Dollodon bampingi* (Norman 1986, fig. 53), *Eolambia caroljonesa* (Kirkland 1998), *Iguanodon bernissartensis* (Norman 1980, fig. 63) and *Tethyshadros insularis* (Dalla Vecchia 2009) by the absence of a prominent overhanging dorsal margin above the ischial peduncle (the supraacetabular process). The presence of a brevis shelf and fossa that is visible in lateral view distinguishes *Jinzhousaurus* from *Altirhinus kurzanovi* (Norman 1998, fig. 32), *Dollodon bampingi* (Norman 1986, fig. 53), *Iguanodon bernissartensis* (Norman 1980, fig. 63), *Mantellisaurus atherfieldensis* (Hooley 1925), *Ouranosaurus nigeriensis* (Taquet 1976, fig. 58), at least some individuals of *Probactrosaurus gobiensis* (Norman 2002, fig. 27B), and *Tethyshadros insularis* (Dalla Vecchia 2009). *Jinzhousaurus* lacks the strongly downturned preacetabular process seen in *Iguanodon bernissartensis* (Norman 1980, fig. 63) and *Mantellisaurus atherfieldensis* (Hooley 1925, fig. 10), and the element is in general proportionally deeper dorsoventrally than the ilium of *I. bernissartensis* or *Dollodon bampingi*. The ilium is unknown in *Fukuisaurus tetoriensis*, *Lanzhousaurus magnidens*, *Nanyangosaurus zhugeii*, '*Probactrosaurus*' *mazongshanensis* and *Protohadros byrdi*. The ilium of *Lurdusaurus arenatus* has been neither figured or described (Taquet & Russell 1999), while the ilium of *Equijubus normani* has been figured (You *et al*. 2003a, fig. 2), but not described.

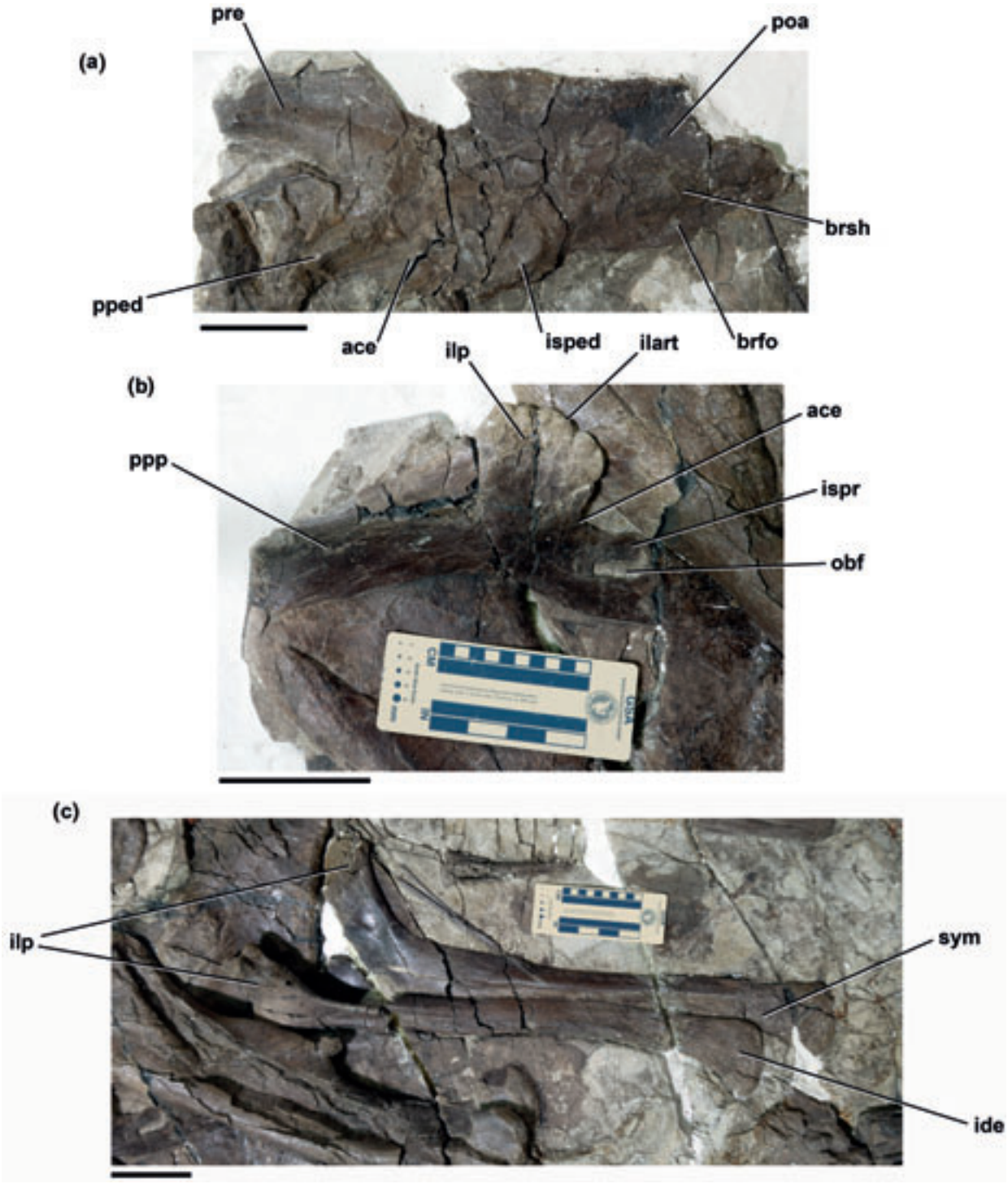

Figure 9 *Jinzhousaurus yangi*, IVPP V12691 (holotype), pelvic girdle: (a) Left ilium, lateral view; (b) Left pubis, lateral view; (c) Left and right ischia. Abbreviations: ace = acetabular margin; brfo = brevis fossa; brsh = brevis shelf; ide = distal expansion of ischium; ilp = iliac peduncle of ischium; isped = ischial peduncle of ilium; ispr = ischial peduncle of pubis; obf = obturator foramen; poa = postacetabular process; pped = pubic peduncle; ppp = prepubic process; pre = preacetabular process; sym = symphysial surface. Scale bars = 10 cm.

2.5.2. Pubis. Only the proximal part of the left pubis is preserved, consisting of the prepubic process and the proximal part of the pubic shaft (Figs 2, 9b). The anterior margin of the prepubic process is damaged.

The prepubic process is a sub-rectangular, transversely compressed plate in lateral view (Fig. 9b: ppp). Its posterior margin is slightly expanded dorsoventrally with respect to its central and anterior portions, such that it increases in depth posteriorly. The anterior end of the prepubic process is broken, and so it is not possible to determine if it was dorsoventrally expanded, as occurs in other non-hadrosaurid iguanodontians. The lateral surface of the prepubic process is gently concave both dorsoventrally and anteroposteriorly and the medial surface is gently convex anteroposteriorly. At its posterior end the prepubic process is expanded to form a posterodorsal projection, the iliac peduncle (Fig. 9b: ilp), which contacted the pubic peduncle of the ilium. The articular surface for the ilium (Fig. 9b: ilart) is transversely expanded anteriorly but thins posteriorly, giving the surface an elongate sub-triangular outline. This surface is very strongly rugose in dorsal and lateral views, and gently convex in lateral view. In lateral view, the posterior margin of the iliac peduncle curves ventrally and

merges with the dorsal margin of the ischial peduncle, forming the pubic contribution to the acetabular margin (Fig. 9b: ace). The ischial peduncle is a short, finger-like structure that extends posteroventrally from the proximal pubic plate and forms the posterior margin of the elliptical obturator foramen (Fig. 9b: ispr). Poor preservation in this area means that it is not possible to determine if the obturator foramen (Fig. 9b: obf) was fully enclosed by bone or was open posteriorly. Other details of the ischial peduncle are obscured by overlying elements. The pubic shaft extends posteroventrally from the prepubic process and runs parallel to the ischiac peduncle.

The incomplete preservation and exposure of the pubes of *Jinzhousaurus* limits comparisons. The pubis of *Camptosaurus* is generally similar to the preserved morphology in *Jinzhousaurus* (Carpenter & Wilson 2008, fig. 29), but the articular surface for the ilium is not as strongly rugose, nor is it as strongly offset from the ischial peduncle. The pubis of *Ouranosaurus gobiensis* (Taquet 1976, fig. 58) is distinct in possessing a prepubic process proportionally deeper at its base and that is offset in lateral view from the iliac peduncle, rather than merging smoothly with it as occurs in *Jinzhousaurus*. In *Iguanodon bernissartensis* the obturator opening is reduced in size and subcircular (Norman 1980, fig. 64), rather than elliptical as occurs in *Jinzhousaurus*. A similarly reduced obturator foramen is also present in *Altirhinus kurzanovi* (Norman 1998, fig. 33) and *Lurdusaurus arenatus* (Taquet & Russell 1999, pl. 3, fig. 1). Although the anterior end of the prepubic process is incomplete, it seems unlikely that *Jinzhousaurus* possessed a deeply flared process similar to that of *Dollodon bampingi* (Norman 1986, fig. 55), *Lanzhousaurus magnidens* (You *et al*. 2005, fig. 3C), *Mantellisaurus atherfieldensis* (Hooley 1925, fig. 10) and *Probactrosaurus gobiensis* (Norman 2002, fig. 28), in which the dorsoventral expansion begins at the midpoint of the length of the process. Pubes of other Asian non-hadrosaurid iguanodontians are either unknown or unfigured, preventing further comparisons.

2.5.3. Ischium. Both ischia are preserved (Figs 2, 9c). The left ischium is visible in posterolateral view and some details of the medial surface of the proximal end can be observed. The right ischium is visible in medial view only. The anterior part of the proximal plate of the right ischium is broken and has become detached from the rest of the element.

The ischium consists of an anteroposteriorly expanded proximal plate and an elongate shaft that arises from the posteroventral corner of the proximal end. The transversely compressed proximal plate has a subrectangular main body that supports the pubic and iliac peduncles anterodorsally and posterodorsally. The iliac peduncle (Fig. 9c: ilp) is strongly expanded transversely relative to the main body. In lateral view, the surface of the proximal plate is gently concave anteroposteriorly, with anterior and posterior margins that are thickened to form dorsoventrally extending ridges that buttress both pubic and iliac peduncles. The cross-sectional outline of the pubic peduncle and its articular surface cannot be determined in either ischium, due to the presence of other overlying bones. The acetabular margin is visible on the left ischium and is gently concave in lateral view. The iliac articular surface has an elliptical cross-sectional outline and is shallowly concave on the right ischium. By contrast, the left iliac peduncle has an irregular articular surface marked by large, possibly pathological, calluses of bone.

In lateral view, the ischial shaft is straight to slightly arched dorsally along its length. It maintains an approximately constant thickness along its length, except for the distal end, which is expanded anteroposteriorly, to produce a sub-triangular termination in lateral view (Fig. 9c: ide). Due to the orientation in which the ischia are preserved, it is not possible to determine if an obturator process is present on the ventral margin of the shaft. A prominent ridge extends longitudinally along the medial surface of the shaft, possibly from the base of the obturator process, as occurs in other non-hadrosaurid iguanodontians (e.g., Norman 1998, 2002); as a result, the shaft at midlength has a sub-triangular cross-section. This ridge defines the posterior margin of a strongly striated sub-triangular surface on the medial surface of the distal end of the bone (Fig. 9c: sym): this surface represents the ischial symphysis where the element was in contact with its opposite.

The ischium is similar in morphology to the equivalent elements in many other non-hadrosaurid iguanodontians, including *Camptosaurus dispar* (Carpenter & Wilson 2008, fig. 28), *Iguanodon bernissartensis* (Norman 1980, figs 64, 67), *Mantellisaurus atherfieldensis* (Hooley 1925, fig. 10), *Nanyangosaurus zhugeii* (Xu *et al*. 2000, fig. 1F), *Ouranosaurus nigeriensis* (Taquet 1976, fig. 60), *Probactrosaurus gobiensis* (Norman 2002, fig. 29) and an ischium of a juvenile individual referred to *Eolambia caroljonesa* (Kirkland 1998: fig. 8C). The ischium of *Jinzhousaurus* differs from that referred to *Eolambia caroljonesa* (Kirkland 1998, fig. 8A) in lacking a very strong distal expansion with a sub-rectangular outline. The ischium of *Tethyshadros* differs from *Jinzhousaurus* in being unexpanded at its distal end (Dalla Vecchia 2009). Taquet & Russell (1999) did not figure the ischium of *Lurdusaurus arenatus*, but it is described as possessing an expanded distal end and a ''strongly recurved'' shaft (Taquet & Russell 1999, p. 90). The ischium is unknown in other Asian iguanodontians.

2.6. Hindlimb

2.6.1. Femur. Both femora are present (Figs 2, 10): the right femur is visible in anterior view while the left femur is visible in lateral view. The lateral surface of the left femur is badly damaged; the preservation of the right femur is better, but its proximal end is obscured by the pubis.

The femur is a columnar element in lateral and anterior views and bears a dorsomedially protruding head. The finger-like anterior trochanter (Fig. 10: ltr) is closely appressed to the greater trochanter (Fig. 10: gtr) and is separated from it by a narrow groove. The anterior trochanter terminates slightly below the level of the greater trochanter. A pendant and blade-shaped fourth trochanter is present on the posteromedial margin of the femur situated at approximately the midlength of the shaft (Fig. 10: ftr). The distal end of the femur is slightly expanded transversely and strongly expanded anteroposteriorly with respect to the shaft. In anterior view, a deep and narrow extensor intercondylar groove extends proximodistally along the midline of the distal shaft (Fig. 10: aigr), dividing the lateral and medial condyles ventrally. This groove is partially enclosed by extensions of the bone surface from either side of the groove. Although largely obscured, the distal articular surfaces are strongly rugose. Posteriorly, each distal condyle supports a sub-rectangular epicondyle; these epicondyles are separated on the midline by a deep flexor sulcus (Fig. 10: pigr). The lateral (fibular) epicondyle is inset from the lateral surface of the femur (Fig. 10: lepi) and is narrower in transverse width than the medial (tibial) epicondyle.

The morphology of the femur of *Jinzhousaurus* cannot be distinguished from that of several other non-hadrosaurid iguanodontians, including *Iguanodon bernissartensis* (Norman 1980, fig. 68), *Mantellisaurus atherfieldensis* (Hooley 1925, fig. 9), *Nanyangosaurus zhugeii* (Xu *et al*. 2000, fig. 2G), *Probactrosaurus gobiensis* (Norman 2002, fig. 30) and '*Probactrosaurus*' *mazongshanensis* (Lü 1997, fig. 10). However, the femur of *Jinzhousaurus* does appear to be considerably more robust relative to its length than the femora of *Dollodon bampingi* (Norman 1986, fig. 57A, B) and *Ouranosaurus*

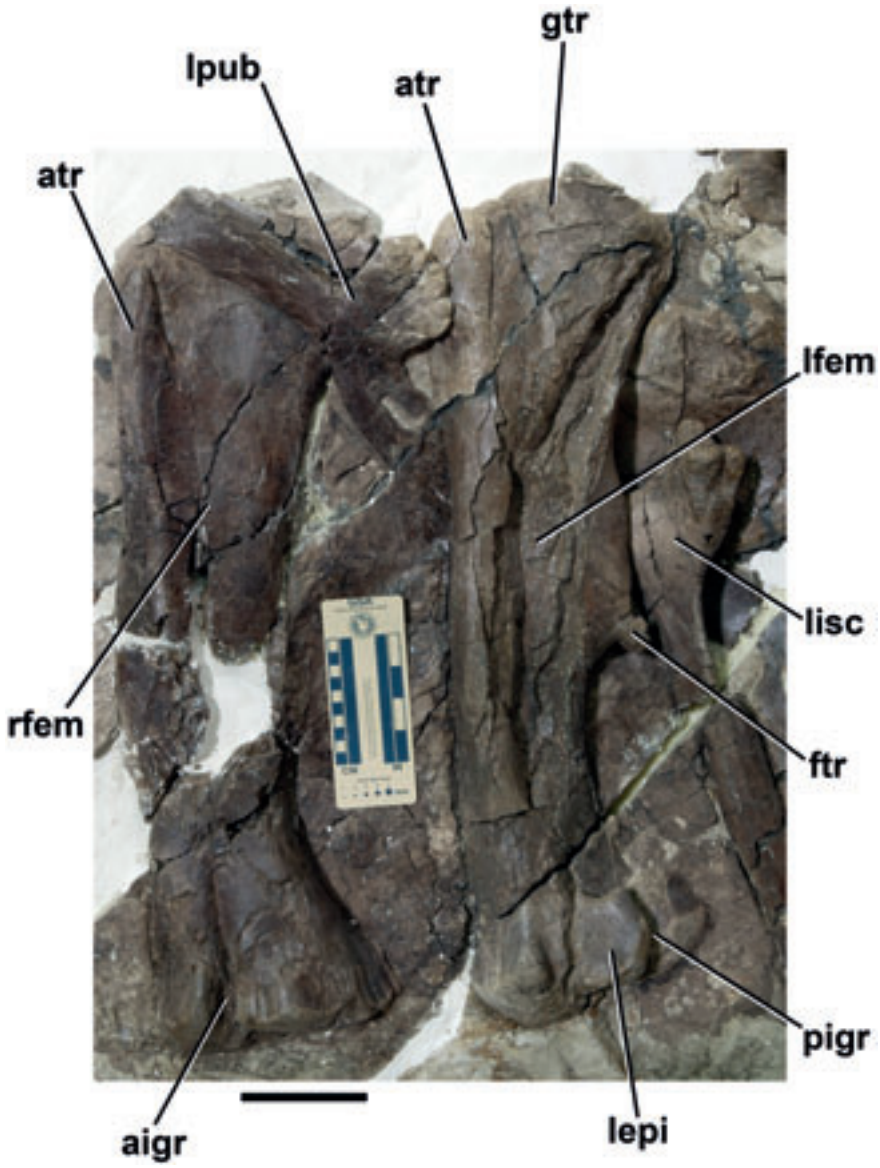

Figure 10 *Jinzhousaurus yangi*, IVPP V12691 (holotype), femora. Abbreviations: aigr=anterior intercondylar groove; atr=anterior trochanter; ftr=fourth trochanter; gtr=greater trochanter; lepi=lateral epicondyle; lfem=left femur; lisc=left ischium; lpub=left pubis; pigr=posterior intercondylar groove; rfem=right femur. Scale bars=10 cm.

nigeriensis (Taquet 1976, fig. 62). The femur is unknown in *Equijubus normani*, *Fukuisaurus tetoriensis* and *Lanzhousaurus magnidens*, and incompletely known or undescribed in *Altirhinus kurzanovi*, *Eolambia caroljonesa*, and *Lurdusaurus arenatus*.

2.6.2. Tibia & fibula. Both tibiae and fibulae are present, but are so badly crushed they offer almost no useful anatomical information (Fig. 2). All that can be said about the tibia is that it is a columnar element that consists of a transversely expanded distal end and a long sub-cylindrical shaft. The distal end is separated into medial and lateral malleoli and is subtriangular in distal view with the apex of the triangle formed by a proximally extending ridge on the posterior surface. The fibulae are so badly preserved they can only be identified on the basis of their association with the tibiae and the fact that they were elongate rod-like elements. There is an isolated proximal fibula distal to the remaining elements – it is expanded anteroposteriorly and has a subtriangular outline in lateral view. The exceptionally poor preservation of these elements precludes both measurements and comparison with other non-hadrosaurid iguanodontians.

2.6.3. Pedal phalanx. An isolated phalanx, visible in distal view, is the only pedal element preserved. The proximodistal length of the element is relatively short, suggesting that it is one of the more distally positioned phalanges, and has a saddle-shaped distal articular surface that is wider than high. No additional details can be determined.

3. Phylogenetic analysis

Jinzhousaurus has been included in three previous phylogenetic analyses, although in the first two cases it was scored only on the basis of the cranial descriptions presented by Wang & Xu (2001a, b). You *et al.* (2003a, fig. 3) included *Jinzhousaurus* within an analysis of 15 taxa and 66 characters, scoring this taxon for only 50% of these characters. *Jinzhousaurus* was placed within a polytomy at the base of Ankylopollexia, along with Iguanodontidae (including *Iguanodon*, *Ouranosaurus* and *Altirhinus*) and Hadrosauroidea (including *Equijubus*, *Probactrosaurus*, *Bactrosaurus*, *Protohadros*, *Telmatosaurus* and Hadrosauridae). Norman (2004) carried out two phylogenetic

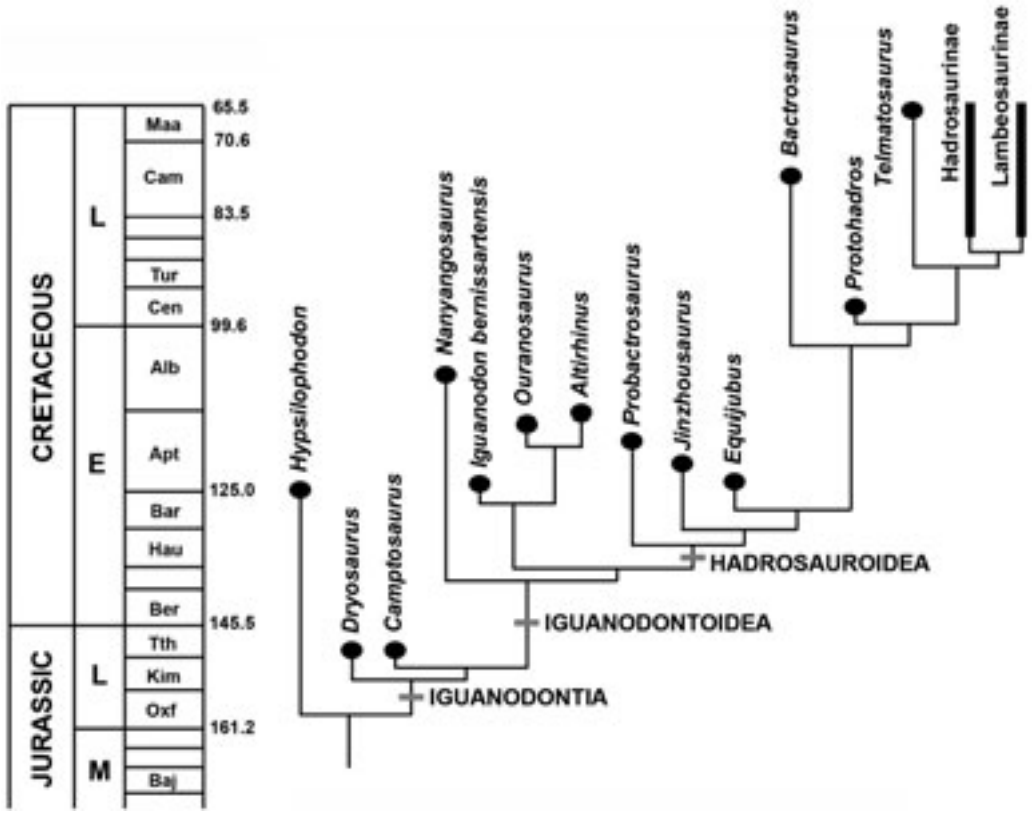

Figure 11 Single most parsimonious tree resulting from analysis of the modified cladistic data matrix of You *et al.* (2003a), calibrated stratigraphically.

analyses of iguanodontians. The first analysis included 21 taxa, including *Jinzhousaurus* (scored for just 27% of characters), and 67 characters, and placed *Jinzhousaurus* in a polytomy (along with *Probactrosaurus*, *Nanyangosaurus* and *Bactrosaurus*+*Edmontosaurus*) within Hadrosauroidea, in a more derived position than *Protohadros* (Norman 2004, fig. 19.21). This proposed position is more derived than that suggested by You *et al.* (2003a). Subsequently, Norman (2004) pruned five taxa, including *Jinzhousaurus*, and reran the analysis, recovering a topology that differed only slightly from the more taxonomically inclusive analysis. Finally, Prieto-Marquez (2010) included *Jinzhousaurus* in his large analysis (56 taxa, 288 characters) of hadrosauroids, placing it as the most basal member of Hadrosauroidea.

Although a full revision of iguanodontian phylogeny is beyond the scope of this present contribution, the matrices of You *et al.* (2003a) and Norman (2004) have been reanalysed, incorporating new data on the cranial and postcranial morphology of *Jinzhousaurus*. The analysis of Prieto-Marquez (2010) was not considered, because it is focused on more derived hadrosauroids. Scores for all taxa other than *Jinzhousaurus* were left unchanged in the matrices of You *et al.* (2003a) and Norman (2004). For the matrix of You *et al.* (2003a), an additional character state was added to character 54 (ungual of manual digit I is subequal in length to that of digit II). Scores for *Jinzhousaurus* are provided in Appendix 2. It is noted that in the published data matrix provided by You *et al.* (2003a), the character scores for characters 63 and 64 appear to have been reversed. The present authors score *Jinzhousaurus* as '1' for character 63 and '?' for character 64, as listed by You *et al.* (2003a: table 1). A copy of the modified matrix is available from RJB on request. For the matrix of Norman (2004), character 9 in the character list appears to be misworded, and actually refers to the presence or absence of a contact between the lacrimal and nasal (not the lacrimal and maxilla, as worded). *Jinzhousaurus* was scored for 70% of characters for the matrix of You *et al.* (2003a) and 76% of characters for the matrix of Norman (2004).

Both matrices were reanalysed in PAUP* 4.0b10 (Swofford 2002), using branch-and-bound searches with all characters unordered and equally weighted. For the matrix of You *et al.* (2003a), a single most parsimonious tree (MPT) of 113 steps was recovered (Fig. 11). *Jinzhousaurus* is placed within Hadrosauroidea, as more closely related to *Equijubus*, *Bactrosaurus*, *Protohadros* and hadrosaurids than to *Probactrosaurus* or Iguanodontidae (*Iguanodon* + *Altirhinus*+*Ouranosaurus*). This is a more derived position than recovered by You *et al.* (2003a), and the character scores for *Jinzhousaurus* have also impacted on the position of *Probactrosaurus*, which is positioned more basally than previously. Hadrosauroidea is supported by the following unambiguous synapomorphies in this analysis: ventral margin of premaxilla convex (character 9, state 1); articular surface of occipital condyle inclined vertically (character 24, state 1; unknown in *Jinzhousaurus*); basipterygoid process elongate (character 25, state 1; unknown in *Jinzhousaurus*); two replacement teeth per dentary tooth family (character 33, state 1; unknown in *Jinzhousaurus*); dentary teeth larger than the maxillary teeth (character 34, state 1). The position of *Jinzhousaurus* closer to hadrosaurids than to *Probactrosaurus* is supported by the strong ventral deflection of the oral margin of the premaxilla below the dentary tooth row (character 8, state 2) and the presence of a mandibular diastema (character 26, state 1).

Reanalysis of the matrix of Norman (2004) recovered 126 MPTs of 142 steps. The strict component consensus of these trees (Fig. 12) is very similar to that presented by Norman (2004, fig. 19.21), with the key difference that *Jinzhousaurus* is placed close to the base of Hadrosauroidea, in a polytomy that contains *Jinzhousaurus*, *Mantellisaurus atherfieldensis*, and hadrosauroids. In 50% of the MPTs, *Jinzhousaurus* is

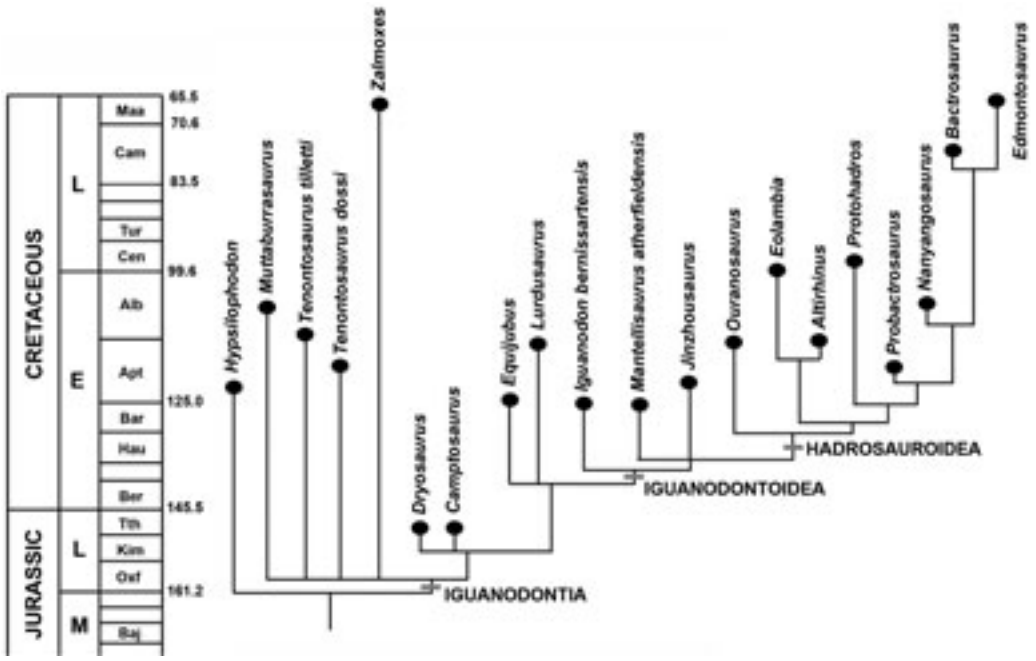

Figure 12 Strict component consensus of 63 most parsimonious trees resulting from analysis of the modified cladistic matrix of Norman (2004), calibrated stratigraphically.

recovered as the most basal hadrosauroid (however, this position is supported by no unambiguous synapomorphies), whereas the remaining 50% of the MPTs contain the same polytomy as the consensus tree. In addition, relationships among basal iguanodontians are poorly resolved when compared to the result presented by Norman (2004). This position for *Jinzhousaurus* differs considerably from that reported by Norman (2004, fig. 19.21), in which *Jinzhousaurus* was placed much closer to Hadrosauridae. Norman (2004) scored *Jinzhousaurus* based on the brief description of Wang & Xu (2001b), which focused on the skull only, and was only scored for 27% of the characters. This high percentage of missing data appears to have resulted in *Jinzhousaurus* acting as an unstable 'wildcard' taxon in the analysis of Norman (2004). The incorporation in the present paper of more complete cranial and postcranial data supports a more basal position for *Jinzhousaurus*.

Major incongruities exist between the results of the two analyses (e.g., the positions of *Altirhinus* and *Probactrosaurus*), but both analyses place *Jinzhousaurus* close to the base of Hadrosauroidea, possibly as one of its earliest known members. This result is in keeping with the relatively early stratigraphic appearance (lower Aptian) of *Jinzhousaurus*, which is similar to the Barremian–Aptian age of *Iguanodon bernissartensis* and *Mantellisaurus atherfieldensis*. Character and taxon sampling remains relatively low in available phylogenetic analyses of non-hadrosaurid iguanodontians, and more detailed work is needed in this area in the future in order to provide more clearly resolved relationships. Future progress in this area requires a more stable taxonomic framework (particularly for the multiple species previously referred to the genus *Iguanodon*: Paul 2006, 2008; Norman in press), careful redescriptions of a number of key taxa (such as that presented here), and a detailed review of the definitions and distribution of all previously proposed phylogenetic characters.

4. Ontogenetic stage, body size and posture

Although histological analyses have not been carried out, the complete closure of the sutures between the neural arches and centra throughout the vertebral column (where visible) is suggestive of skeletal maturity in the holotype specimen of *Jinzhousaurus*. As discussed above, a body length of 5–5·5 m is estimated for this individual, which is not particularly large by the standards of non-hadrosaurid iguanodontians. The femoral length (630 mm) is shorter than that of some closely related taxa such as *Dollodon bampingi* (760 mm: Norman 1986) and *Iguanodon bernissartensis* (1030 mm for the holotype specimen: Norman 1986), *Lurdusaurus arenatus* (910 mm: Taquet & Russell 1999), *Ouranosaurus nigeriensis* (850 mm: Taquet 1976), and '*Probactosaurus*' mazongshanensis (estimated at 1000 mm; Lü 1997). However, it appears comparable in size to, or moderately larger than, taxa such as *Mantellisaurus atherfieldensis* (678 mm: Hooley 1925) and *Nanyangosaurus zhugeii* (517 mm: Xu *et al.* 2000). Comparisons with mass estimates for other similar-sized non-hadrosaurid iguanodontians (Seebacher 2001) suggest a body mass of 0·5–1 tonne for *Jinzhousaurus*.

Assessment of the relative proportions of fore- and hindlimbs in *Jinzhousaurus* is complicated by the poor preservation of the tibia/fibula, and the absence of the metatarsus and pes. However, the humerus is ~67% the length of the femur, which is intermediate between the shortened forelimbs seen in *Dollodon bampingi* and *Mantellisaurus atherfieldensis* (humerus is 58% and 56% femoral length, respectively; see above) and the extremely elongate forelimbs seen in *Iguanodon bernissartensis* (humerus is 77–80% femoral length; see above). These limb proportions suggest that *Jinzhousaurus* may have been a facultive quadruped, as in many other non-hadrosaurid iguanodontians (Norman 2004).

5. Conclusions

The holotype specimen of *Jinzhousaurus yangi* is the most complete of any Asian non-hadrosaurid iguanodontian, allowing the morphology of the postcranial skeleton to be documented in detail. Only fragmentary and highly incomplete postcranial material is known for most other Asian taxa (e.g., Lü 1997; Xu *et al.* 2000; You *et al.* 2003a, b, 2005). Two

autapomorphies of *Jinzhousaurus* are recognised (the morphology of the sternal and the short manual phalanges) based upon postcranial material; moreover, many postcranial elements can be distinguished from those of other non-hadrosaurid iguanodontians on the basis of a unique combination of characters. These observations, combined with the large number of previously recognised cranial autapomorphies (Barrett *et al*. 2009), provide strong support for the validity of *Jinzhousaurus*. Although the postcranial skeletons of non-hadrosaurid iguanodontians are often considered conservative, significant taxonomically and phylogenetically informative variation does occur between species, and recent cladistic data matrices for Iguanodontia include up to 45% postcranial characters (e.g., Norman 2002, 2004). Detailed documentation of the postcranial morphology of non-hadrosaurid iguanodontians is therefore fundamental to future investigations of non-hadrosaurid iguanodontian taxonomy and phylogeny.

6. Acknowledgements

We would like to thank Xinzheng Liu, Long Xiang and Fulin Wang for the preparation of the specimen and Wei Gao for the photos. The drawings in Figures 2, 6 and 7 were provided by Robert Laws, based in part upon original drawings by Minwan Yang and Jinling Huang. We thank Zhonghe Zhou, Xing Xu, Yuan Wang and Jiangjong Zhang for their help and discussions. Qiang Wang provided much assistance during the course of this research. This study was supported by National Natural Science Foundation of China (40121202), The Major Basic Research Projects of the Ministry of Science and Technology of China (2006CB806400) and the National Science Fund for Distinguished Young Scholars (40825005). The travel of RJB to China was supported in part by a Predoctoral Fellowship from the Society of Vertebrate Paleontology and a Systematics Association Research Grant. RJB was supported during the completion of this research by an Alexander von Humboldt Research Fellowship. PMB was funded by the Royal Society and the Hodson Award of the Palaeontological Association (UK). We thank David Norman for making the original matrix of Norman (2004) available to us, and Graeme Lloyd (NHMUK) for providing a copy of the matrix of You *et al*. (2003a) via his website. Reviews by David Weishampel and Pascal Godefroit improved the final manuscript. This represents Publication Number 1 under the new Memorandum of Understanding between IVPP and NHMUK. PMB publishes with the permission of The Natural History Museum, London.

7. Appendix 1: Measurements

7.1. Axial column

Maximal length of neural arch of the atlas = 70 mm

Maximal length of neural arch of the axis = 108 mm

Cervical 3 (ventral exposure): length of centrum = 55·5 mm; anterior width of centrum = 71·5 mm; posterior width of centrum = 69 mm [Note that all centrum lengths for the cervical vertebrae exclude the convexity on the anterior articular surface]

Cervical 4 (lateral exposure): length of centrum (dorsal) = 56·5 mm; length of centrum (ventral) = 63·5 mm; anterior height of centrum = 66·5 mm; posterior height of centrum = 73 mm

Cervical 5 (lateral exposure): centrum length (dorsal) = 56 mm; centrum length (ventral) = 60 mm; centrum height (anterior) = 69 mm; centrum height (posterior) = 69·5 mm

Cervical 6 (lateral exposure): centrum length (dorsal) = 55 mm; centrum length (ventral) = 59 mm; centrum height (anterior) = 62 mm; centrum height (posterior) = 74 mm

Cervical 7 (lateral exposure): centrum length (ventral) = 59 mm; centrum height (posterior) = 73 mm

Cervical 8 (lateral exposure): centrum height (posterior) = 74·5 mm

Cervical 9 (lateral exposure): centrum length (dorsal) = 60 mm; centrum length (ventral) = 61 mm; centrum height (anterior) = 63·5 mm; centrum height (posterior) = 71·5 mm

Cervical 10 (lateral exposure): centrum length (dorsal) = 55 mm; centrum length (ventral) = 56·5 mm; centrum height (anterior) = 67·5; centrum height (posterior) = 67·5 mm

No measurements are available for cervical 11

Cervical rib length, measured from capitulum to shaft tip: cervical rib 4 = 60 mm; cervical rib 5 = 65 mm; cervical rib 8 ~ approx 73 mm; cervical rib 9 = 77 mm; cervical rib ?11 = 117 mm

Dorsal '1': anterior width of centrum = 60 mm; anterior height of centrum = 60 mm

Dorsal '4': posterior width of centrum = 70 mm; posterior height of centrum = 57 mm; total height of vertebra, including neural arch = 192 mm

Dorsal '5': anterior width of centrum ~ 50 mm; anterior height of centrum = 66 mm; centrum length = 63 mm

Dorsal '7': posterior width of centrum = 68 mm; posterior height of centrum = 74 mm; centrum length: 53 mm

Dorsal '8': posterior height of centrum = 76 mm; centrum length = 61·5 mm

Dorsal '9': posterior height of centrum = 79 mm

Dorsal '12': anterior height of centrum = 78 mm; posterior height of centrum = 90 mm; centrum length = 57 mm; total height of vertebra = 252 mm

Caudal '1': anterior width of centrum = 89 mm; anterior height of centrum = 59 mm

Caudal '2': anterior width of centrum = 86 mm; anterior height of centrum = 67 mm; total height of vertebra = 245 mm

Caudal '3': anterior width of centrum = 81 mm; anterior height of centrum = 67 mm; total height of vertebra = 250 mm

Caudal '4': posterior width of centrum = 77 mm; posterior height of centrum = 78 mm; centrum length = 48 mm; total height of vertebra = 235 mm

Caudal '5': posterior width of centrum = 70 mm; posterior height of centrum = 72 mm; centrum length = 46 mm

Caudal '6': anterior width of centrum = 67 mm; anterior height of centrum = 69 mm; total height of vertebra = 215 mm

Caudal '7': posterior width of centrum = 71 mm; posterior height of centrum = 63 mm; centrum length = 54 mm

Caudal '8': anterior width of centrum = 59 mm; anterior height of centrum = 52 mm; posterior height of centrum = 62 mm; centrum length = 57 mm; total height of vertebra = 165 mm

Caudal '9': posterior height of centrum = 65 mm; centrum length = 53 mm; total height of vertebra = 153 mm

Caudal '10': posterior height of centrum = 62 mm; centrum length = 55 mm; total height of vertebra = 145 mm

Caudal '11': posterior height of centrum = 67 mm; centrum length = 52 mm; total height of vertebra = 156 mm

Caudal '12': posterior height of centrum = 61 mm; centrum length = 57 mm; total height of vertebra = 150 mm

Caudal '13': centrum length = 51 mm; total height of vertebra = 130 mm

7.2. Appendicular elements

Scapula, left: total length = 504 mm; dorsoventral depth of distal expansion = 139 mm; minimum dorsoventral depth of shaft = 76 mm; maximal dorsoventral depth of proximal expansion = 150 mm

Coracoid, left: anteroposterior length = 13·5 cm; maximal dorsoventral height = 145 mm
Sternal: maximal length (along ventrolateral process) = 240 mm; maximal transverse width = 89 mm; maximal length (along midline) = 175 mm
Humerus, left: length = 420 mm; transverse width of proximal end = 132 mm; transverse width of distal end = 108 mm; minimum transverse width at midshaft = 56 mm
Humerus, right: length = 42 cm; minimum transverse width at midshaft = 61 mm
Ulna: length (as preserved) = 325 mm; maximum width of proximal expansion = 69 mm; minimum width at midshaft = 41·5 mm
Radius: length = 265 mm; anteroposterior width of proximal end = 56·5 mm; anteroposterior width of distal end: 62·5 mm; minimum width at midshaft = 34 mm Metacarpal 2, left: length = 84 mm
Metacarpal 3, left: length = 112 mm
Metacarpal 4, left: length = 97 mm
Metacarpal 5, left: length = 50 mm
Phalanx 1–2, left: length = 56 mm (incomplete)
Phalanx 1–2, right: length = 81 mm; transverse width at proximal end = 33 mm
Phalanx 2–1, left: length = 26 mm; transverse width at proximal end = 33·5 mm
Phalanx 2–2, left: length = 12·5 mm; transverse width at proximal end = 32 mm
Phalanx 2–3, left: length = 82 mm; transverse width at proximal end = 36 mm
Phalanx 2–3, right: length = 79 mm
Phalanx 3–1, left: length = 18·5 mm; transverse width at proximal end = 35·5 mm
Phalanx 3–2, left: length = 10 mm; transverse width at proximal end = 29·5 mm
Phalanx 3–3, left: transverse width at proximal end = 40 mm
Phalanx 4–1, left: length = 22 mm; transverse width at proximal end = 26 mm
Phalanx 5–1, left: length = 42·5 mm; transverse width at proximal end = 29 mm
Ilium, left: length (as preserved) = 512 mm
Pubis: anteroposterior length of prepubic process (as preserved) = 232 mm
Ischium, left: length of shaft (from the base of the proximal plate) = 560 mm; total length (from iliac peduncle to end of shaft) = 690 mm
Ischium, right: length of shaft (from the base of the proximal plate) = 550 mm; total length (from iliac peduncle to end of shaft) = 645 mm Femur, right: length = 630 mm
Femur, left: length = 620 mm

8. Appendix 2: cladistic scores for *Jinzhousaurus*

Matrix of You *et al.* (2003a) (score in bold indicates that it was rescored from that given by You *et al.* 2003a): 011**11**10021**?** 020**?1**0000? **??**????**1**0010 01**?1**100**20?** ????**111111 1112111?1**? ??**1**??**0**

Matrix of Norman (2004) (score in bold indicates that it was rescored from that given by Norman 2004): 01**?1012–1**0 **0**?1?110**?01** 01**?**000**011**? ?**10110?1?2 0110110111** ?**0101**??**01**? **1?120**??

9. References

Barrett, P. M., Butler, R. J., Wang, X.-L. & Xu, X. 2009. Cranial anatomy of *Jinzhousaurus yangi* (Dinosauria, Ornithopoda) from the Yixian Formation (Lower Cretaceous) of China. *Acta Palaeontologica Polonica* **54**, 35–48.

Butler, R. J. 2005. The 'fabrosaurid' ornithischian dinosaurs of the Upper Elliot Formation (Lower Jurassic) of South Africa and Lesotho. *Zoological Journal of the Linnean Society* **145**, 175–218.

Calvo, J. O., Porfiri, J. D. & Novas, F. E. 2007. Discovery of a new ornithopod dinosaur from the Portezuelo Formation (Upper Cretaceous), Neuquén, Patagonia, Argentina. *Arquivos do Museu Nacional, Rio de Janeiro* **75**, 471–83.

Carpenter, K. & Wilson, Y. 2008. A new species of *Camptosaurus* (Ornithopoda: Dinosauria) from the Morrison Formation (Upper Jurassic) of Dinosaur National Monument, Utah, and a biomechanical analysis of its forelimb. Annals of the Carnegie Museum **76**, 227–63.

Chen, J., Butler, R. J. & Jin, L. 2008. New material of large-bodied ornithischian dinosaurs, including an iguanodontian ornithopod, from the Quantou Formation (middle Cretaceous: Aptian–Cenomanian) of Jilin Province, northeastern China. *Neues Jahrbuch für Geologie und Paläontologie, Abhandlungen* **248**, 309–14.

Cope, E. D. 1869. Synopsis of the extinct Batrachia, Reptilia, and Aves of North America. *Transactions of the American Philosophical Society* **14**, 1–252.

Dalla Vecchia, F. M. 2009. *Tethyshadros insularis*, a new hadrosauroid dinosaur (Ornithischia) from the Upper Cretaceous of Italy. *Journal of Vertebrate Paleontology* **29**, 1100–16.

Galton, P. M. 1974. The ornithischian dinosaur *Hypsilophodon* from the Wealden of the Isle of Wight. *Bulletin of the British Museum* (*Natural History*) *Geology* **25**, 1–152c.

Gilmore, C. W. 1909. Osteology of the Jurassic reptile *Camptosaurus*, with a revision of the species of the genus, and description of two new species. *Proceedings of the United States National Museum* **41**, 197–332.

Gilmore, C. W. 1933. On the dinosaurian fauna of the Iren Dabasu Formation. *Bulletin of the American Museum of Natural History* **67**, 23–78.

Godefroit, P., Dong, Z., Bultynk, P., Li, H. & Feng, L. 1998. New *Bactrosaurus* (Dinosauria: Hadrosauroidea) material from Iren Dabasu (Inner Mongolia, P.R. China). *Bulletin de l'Institut Royal des Sciences Naturelles de Belgique. Sciences de la Terre* **68** (Suppl.), 3–70.

Godefroit, P., Li, H. & Shang, C.-Y. 2005. A new primitive hadrosauroid dinosaur from the Early Cretaceous of Inner Mongolia (P.R. China). *Comptes Rendus Palevol* **4**, 697–705.

Head, J. J. 1998. A new species of basal hadrosaurid (Dinosauria, Ornithischia) from the Cenomanian of Texas. *Journal of Vertebrate Paleontology* **18**, 718–38.

Hooley, R. W. 1925. On the skeleton of *Iguanodon atherfieldensis* sp. nov., from the Wealden Shales of Atherfield (Isle of Wight). *Quarterly Journal of the Geological Society; London* **81**, 1–61.

Kirkland, J. I. 1998. A new hadrosaurid from the upper Cedar Mountain Formation (Albian–Cenomanian: Cretaceous) of eastern Utah – the oldest known hadrosaurid (Lambeosaurine?). *In* Lucas, S. G., Kirkland, J. I. & Estep, J. W. (eds) *Lower and Middle Cretaceous Terrestrial Ecosystems*, 283–95. *New Mexico Museum of Natural History and Science, Bulletin* **14**.

Kobayashi, Y. & Azuma, Y. 2003. A new iguanodontian (Dinosauria: Ornithopoda) from the Lower Cretaceous Kitadani Formation of Fukui Prefecture, Japan. *Journal of Vertebrate Paleontology* **23**, 166–75.

Lü, J.-C. 1997. A new Iguanodontidae (*Probactrosaurus mazongshanensis* sp. nov.) from Mazongshan Area, Gansu Province, China. *In* Dong, Z.-M. (ed.) *Sino–Japanese Silk Road Dinosaur Expedition*, 27–47. Beijing: China Ocean Press.

Marsh, O. C. 1881. Principal characters of American Jurassic dinosaurs. Part IV. Spinal cord, pelvis and limbs of *Stegosaurus*. *American Journal of Science* (*Series 3*) **21**, 167–70.

Mateus, O. & Antunes, M. T. 2001. *Draconyx loureiroi*, a new Camptosauridae (Dinosauria: Ornithopoda) from the Late Jurassic of Lourinhã, Portugal. *Annales de Paleontologie* **87**, 61–73.

Norman, D. B. 1980. On the ornithischian dinosaur *Iguanodon bernissartensis* of Bernissart (Belgium). *Mémoires de l'Institut Royal des Sciences Naturelles de Belgique* **178**, 1–103.

Norman, D. B. 1986. On the anatomy of *Iguanodon atherfieldensis* (Ornithischia: Ornithopoda). *Bulletin de l'Institut Royal des Sciences Naturelles de Belgique, Sciences de la Terre* **56**, 281–372.

Norman, D. B. 1990. A review of *Vectisaurus valdensis*, with comments on the family Iguanodontidae. *In* Carpenter, K. & Currie, P. J. (eds) *Dinosaur Systematics: approaches and perspectives*, 147–61. Cambridge: Cambridge University Press.

Norman, D. B. 1996. On Asian ornithopods (Dinosauria: Ornithischia). 1. *Iguanodon orientalis* Rozhdestvensky, 1952. *Zoological Journal of the Linnean Society* **116**, 303–15.

Norman, D. B. 1998. On Asian ornithopods (Dinosauria: Ornithischia). 3. A new species of iguanodontid dinosaur. *Zoological Journal of the Linnean Society* **122**, 291–348.

Norman, D. B. 2002. On Asian ornithopods (Dinosauria: Ornithischia). 4. *Probactrosaurus* Rozhdestvensky, 1966. *Zoological Journal of the Linnean Society* **136**, 113–44.

Norman, D. B. 2004. Basal Iguanodontia. *In* Weishampel, D. B., Dodson, P. & Osmólska, H. (eds) *The Dinosauria* (2nd edn), 413–37. Berkeley: University of California Press.

Norman, D. B. In press. A taxonomy of iguanodontians (Dinosauria: Ornithopoda) from the lower Wealden Group (Cretaceous: Valanginian) of southern England. *Zootaxa*.

Novas, F. E., Cambiaso, A. V. & Ambrosio, A. 2004. A new basal iguanodontian (Dinosauria, Ornithischia) from the Upper Cretaceous of Patagonia. *Ameghiniana* **41**, 75–82.

Paul, G. S. 2006. Turning the old into the new: a separate genus for the gracile iguanodont from the Wealden of England. *In* Carpenter, K. (ed.) *Horns and Beaks: Ceratopsian and Ornithopod Dinosaurs*, 69–77. Bloomington: Indiana University Press.

Paul, G. S. 2008. A revised taxonomy of the iguanodont dinosaur genera and species. *Cretaceous Research* **29**, 192–216.

Prieto-Marquez, A. 2010. *Glishades ericksoni*, a new hadrosauroid (Dinosauria: Ornithopoda) from the Late Cretaceous of North America. *Zootaxa* **2452**, 1–17.

Prieto-Marquez, A. & Wagner, J. R. 2009. *Pararhabdodon isonensis* and *Tsintaosaurus spinorhinus*: a new clade of lambeosaurine hadrosaurids from Eurasia. *Cretaceous Research* **30**, 1238–46.

Seebacher, F. 2001. A new method to calculate allometric length-mass relationships of dinosaurs. *Journal of Vertebrate Paleontology* **21**, 51–60.

Seeley, H. G. 1887. On the classification of the fossil animals commonly called Dinosauria. *Proceedings of the Royal Society of London* **43**, 165–71.

Sereno, P. C. 1986. Phylogeny of the bird-hipped dinosaurs (Order Ornithischia). *National Geographic Research* **2**, 234–56.

Sereno, P. C. 1998. A rationale for phylogenetic definitions, with application to the higher-level taxonomy of Dinosauria. *Neues Jahrbuch für Geologie und Paläontologie, Abhandlungen* **210**, 41–83.

Sereno, P. C. 1999. The evolution of dinosaurs. *Science* **284**, 2137–47.

Smith, P. E., Evensen, N. M., York, D., Chang, M.-M., Jin, F., Li, J.-L., Cumbaa, S. L. & Russell, D. A. 1995. Dates and rates in ancient lakes: ^{40}Ar–^{39}Ar evidence for an Early Cretaceous age for the Jehol Group, northeast China. *Canadian Journal of Earth Sciences* **32**, 1426–31.

Swisher, C. C. III, Wang, Y.-Q., Wang, X.-L., Xu, X. & Wang, Y. 1999. Cretaceous age for the feathered dinosaurs of Liaoning, China. *Nature* **400**, 58–61.

Swisherk, C. C. III, Wang, X., Zhou Z., Wang, Y., Jin, F., Zhang, J., Xu, X., Zhang, F. & Wang, Y. 2002. Further support for a Cretaceous age for the feathered-dinosaur beds of Liaoning, China: new ^{40}Ar/^{39}Ar dating of the Yixian and Tuchengzi Formations. *Chinese Science Bulletin* **47**, 135–8.

Swofford, D. L. 2002. *PAUP*: Phylogenetic Analysis Using Parsimony* (**and Other Methods*), Version 4. Sunderland, Massachusetts: Sinauer Associates.

Taquet, P. 1976. *Géologie et paléontologie du gisement de Gadoufaoua* (*Aptien du Niger*). Cahiers de Paléontology, Éditions du Centre National de la Recherche Scientifique, Paris. 191 pp+24 pls.

Taquet, P. & Russell, D. A. 1999. A massively-constructed iguanodont from Gadoufaoua, Lower Cretaceous of Niger. *Annales de Paleontologie* **85**, 85–96.

Wang, X.-L. & Xu, X. 2001a. A new iguanodontid (*Jinzhousaurus yangi* gen. et sp. nov.) from the Yixian Formation of western Liaoning, China. *Chinese Science Bulletin* **46**, 419–23. [In Chinese.]

Wang, X.-L. & Xu, X. 2001b. A new iguanodontid (*Jinzhousaurus yangi* gen. et sp. nov.) from the Yixian Formation of western Liaoning, China. *Chinese Science Bulletin* (English translation) **46**, 1669–72.

Wang, X.-L. & Zhou, Z.-H. 2003. Mesozoic Pompeii. *In* Chang, M., Chen, P.-J., Wang, Y.-Q. & Wang, Y. (eds) *The Jehol Biota*, 19–36. Shanghai: Shanghai Scientific & Technical Publishers.

Weishampel, D. B, Jianu, C.-M., Csiki, Z. & Norman, D. B. 2003. Osteology and phylogeny of *Zalmoxes* (N. G.), an unusual euornithopod dinosaur from the latest Cretaceous of Romania. *Journal of Systematic Palaeontology* **1**, 65–123.

Weishampel, D. B., Barrett, P. M., Coria, R. A., Le Loeuff, J., Xu, X., Zhao, X., Sahni, A., Gomani, E. M. P. & Noto, C. R. 2004. *In* Weishampel, D. B., Dodson, P. & Osmólska, H. (eds) *The Dinosauria* (2nd edn), 507–616. Berkeley: University of California Press.

Wiman, C. 1929. Die Kriede-Dinosaurier aus Shantung. *Palaeontologia Sinica, series C* **6**, 1–67.

Xu, X., Zhao, X.-J., Lü, J.-C., Huang, W.-B., Li, Z.-Y. & Dong, Z.-M. 2000. A new iguanodontian from Sangping Formation of Neixiang, Henan and its stratigraphical implication. *Vertebrata PalAsiatica* **38**, 176–91 [In Chinese and English.]

Xu, X. & Norell, M. A. 2006. Non-avian dinosaur fossils from the Lower Cretaceous Jehol Group of western Liaoning, China. *Geological Journal* **41**, 419–37.

You, H.-L., Luo, Z.-X., Shubin, N. H., Witmer, L. M., Tang, Z.-L. & Tang, F. 2003a. The earliest-known duck-billed dinosaur from deposits of Early Cretaceous age in northwest China and hadrosaur evolution. *Cretaceous Research* **24**, 347–55.

You, H.-L., Ji, Q., Li, J. & Li, Y. 2003b. A new hadrosauroid dinosaur from the mid-Cretaceous of Liaoning, China. *Acta Geologica Sinica* **77**, 148–54.

You, H.-L., Ji, Q., and Li, D.-Q. 2005. *Lanzhousaurus magnidens* gen. et sp. nov. from Gansu Province, China: the largest-toothed herbivorous dinosaur in the world. *Geological Bulletin of China* **24**, 785–94.

MS received 21 December 2009. Accepted for publication 3 June 2010.